Retinal Axon Guidance Requires Integration of Eya and the Jak/Stat Pathway into Phosphotyrosine-Based Signaling Circuitries in *Drosophila*

Charlene S. L. Hoi,*,† Wenjun Xiong,*,‡,1 and Ilaria Rebay*,2

*Ben May Department for Cancer Research, †Committee on Genetics, Genomics, and Systems Biology, and ‡Committee on Cancer Biology, University of Chicago, Illinois 60637

ABSTRACT The transcriptional coactivator and phosphatase eyes absent (Eya) is dynamically compartmentalized between the nucleus and cytoplasm. Although the nuclear transcriptional circuits within which Eya operates have been extensively characterized, understanding of its cytoplasmic functions and interactions remains limited. Our previous work showed that phosphorylation of *Drosophila* Eya by the Abelson tyrosine kinase can recruit Eya to the cytoplasm and that *eya–abelson* interactions are required for photoreceptor axons to project to correct layers in the brain. Based on these observations, we postulated that photoreceptor axon targeting might provide a suitable context for identifying the cytoplasmic signaling cascades with which Eya interacts. Using a dose-sensitive *eya* misexpression background, we performed an RNA interference-based genetic screen to identify suppressors. Included among the top 10 hits were nonreceptor tyrosine kinases and multiple members of the Jak/Stat signaling network (*hop*, *Stat92E*, *Socs36E*, and *Socs44A*), a pathway not previously implicated in axon targeting. Individual loss-of-function phenotypes combined with analysis of axonal projections in *Stat92E* null clones confirmed the importance of photoreceptor autonomous Jak/Stat signaling. Experiments in cultured cells detected cytoplasmic complexes between Eya and Hop, Socs36E and Socs44A; the latter interaction required both the Src homology 2 motif in Socs44A and tyrosine phosphorylated Eya, suggesting direct binding and validating the premise of the screen. Taken together, our data provide new insight into the cytoplasmic phosphotyrosine signaling networks that operate during photoreceptor axon guidance and suggest specific points of interaction with Eya.

KEYWORDS SH2; genetic screen; retinal determination network; eye development; Socs44A

A remarkable feature of multicellular animal development is that the complexity and diversity in tissue type and patterning is achieved using fewer than a dozen signaling pathways, including Notch, receptor tyrosine kinase, Wnt, Hedgehog, TGFβ, Jak/Stat, and Hippo. These cascades are repeatedly deployed in different contexts to regulate the majority of the critical proliferation, survival, specification, and differentiation decisions (reviewed in Voas and Rebay 2004; Housden and Perrimon 2014). One strategy to achieve context-specific developmental regulation is for proteins and pathways to function together in interconnected networks. Further, individual proteins within these networks may encode multiple independent functions that can be executed in distinct parts of the cell, cell types, or stages of development. In this way, even a modest number of individual proteins and core pathways can create vast combinatorial possibilities.

Eyes absent (Eya), a protein conserved from plants to humans, presents an ideal model to study integration because its multifunctionality and dynamic subcellular localization provide opportunities for interaction with many signaling pathways (reviewed in Jemc and Rebay 2007 and Tadjuidje and Hegde 2013). In metazoans, Eya has been studied extensively as a transcriptional coactivator and core member of the retinal determination gene network (reviewed in Silver and Rebay 2005 and Kumar 2009). In this context, Eya participates in

doi: 10.1534/genetics.115.185918
Manuscript received December 10, 2015; accepted for publication May 10, 2016; published Early Online May 16, 2016.
Supplemental material is available online at www.genetics.org/lookup/suppl/doi:10.1534/genetics.115.185918/-/DC1.
[1]Present address: Department of Biomedical Sciences, City University of Hong Kong, Kowloon Tong, Hong Kong, China.
[2]Corresponding author: 929 E. 57th St., GCIS W340, Chicago, IL 60637. E-mail: irebay@uchicago.edu

nuclear transcriptional complexes to regulate programs of gene expression that direct cell proliferation, differentiation, and survival in a variety of tissues and organs, including the *Drosophila* eye (Bonini *et al.* 1993, 1998; Pignoni *et al.* 1997; Heanue *et al.* 1999; Ohto *et al.* 1999; Zou *et al.* 2004; Nica *et al.* 2006; Hirose *et al.* 2010). Eya also carries two different phosphatase domains, one with specificity for phosphotyrosine and a second directed toward phosphothreonine (Li *et al.* 2003; Rayapureddi *et al.* 2003; Tootle *et al.* 2003; Okabe *et al.* 2009). Although Eya's tyrosine phosphatase is not required for normal development in *Drosophila* (Jin *et al.* 2013), in mammals it dephosphorylates H2AX to promote repair and survival in response to DNA damage (Cook *et al.* 2009; Krishnan *et al.* 2009) and aPKCζ to direct lung epithelial polarity and morphogenesis (El-Hashash *et al.* 2012). Eya's threonine phosphatase is less well characterized, but appears to act both cytoplasmically to regulate innate immunity and nuclearly to provide transactivation and regulate the activity of other transcription factors (Okabe *et al.* 2009; Liu *et al.* 2012; Xu *et al.* 2014; Jin and Mardon 2016).

Despite increased awareness from mammalian studies of the requirement for Eya function in the cytoplasm, understanding of the specific signaling cascades with which it interacts remains limited. To increase knowledge of the signaling networks with which Eya interfaces, we took advantage of our observation that *Drosophila* Eya can be sequestered in the cytoplasm upon tyrosine phosphorylation (pY) by the Abelson (Abl) kinase (Xiong *et al.* 2009) by performing a genetic modifier screen designed to uncover interactions with genes encoding phosphotyrosine binding proteins. The photoreceptor axon mistargeting phenotypes associated with Eya misexpression provided sensitized backgrounds, and secondary genetic tests allowed us to distinguish interactions likely to impact Eya's cytoplasmic *vs.* nuclear functions. Prominent among the final list of candidate cytoplasmic interactors were several nonreceptor tyrosine kinases and multiple members of the Jak/Stat pathway. Follow-up genetic experiments, including mosaic analysis with a repressible cell marker (MARCM) of *Stat92E* clones, confirmed the pathway is required in the differentiating photoreceptors for axon targeting. To our knowledge, these results provide the first demonstration, either in invertebrates or vertebrates, of a requirement for the Jak/Stat pathway in axon guidance. Focusing on the Jak/Stat pathway factors, we validated the premise of our screen by showing that Eya can be recruited to cytoplasmic complexes via pY–SH2-mediated interactions. Together our results uncover novel requirements for phosphotyrosine-based signaling networks in photoreceptor axon targeting and provide a strong impetus for future mechanistic explorations of how cytoplasmic Eya interfaces with these pathways in both *Drosophila* and mammals.

Materials and Methods

Fly strains

The screen was carried out by crossing RNA interference (RNAi) lines acquired from the Vienna *Drosophila* RNAi Center (VDRC) to five different recombinant stocks containing GMR-Gal4 and Ro-LacZ^{tau}: (1) *GMR-Gal4/CyO-actGFP; Ro-lacZ^{tau}*; (2) *GMR > Eya^{WT}/CyO-actGFP;Ro-lacZ^{tau}*; (3) *GMR > Eya^{RNAi}/CyO-actGFP;Ro-lacZ^{tau}*; (4) *GMR-Gal4/CyO-actGFP;Uas-NLS-Eya^{WT},Ro-lacZ^{tau}/TM6*; and (5) *GMR-Gal4/CyO-actGFP;Uas-Myr-Eya^{WT},Ro-lacZ^{tau}/TM6* (Xiong *et al.* 2009).

UAS-Stat92E and *stat^{85c9}* flies were generously provided by E. Bach. MARCM clones were generated by heat shocking *hsFLP*, *Elav-Gal4*, *UAS-mCD8::GFP;;FRT82B*, *stat^{85c9}/FRT82B*, *tub-Gal80* flies 48 hr after egg laying for 2 hr at 37°.

Socs36E and *Socs44A* RNAi recombinants were confirmed by wing vein phenotypes using the engrailed driver (Rawlings *et al.* 2004b). *upd* and *dome* RNAi lines were acquired from the Bloomington *Drosophila* Stock Center. *UAS-Socs36E* flies were a gift from B. Mathey-Prevot and *UAS-Socs44A* flies were shared by D. Harrison.

Co-immunoprecipitation, immunostaining, and antibodies

Drosophila S2 cells were cultured at 25° in Schneider's medium (Sigma-Aldrich, St. Louis, MO) supplemented with 10% insect medium supplement (Sigma-Aldrich) and penicillin and streptomycin (Invitrogen, Carlsbad, CA). Cells were transfected with 1.0 μg of each plasmid using dimethyldioctadecyl-ammonium bromide (DDAB) (Sigma-Aldrich) transfection and induced with $CuSO_4$. Expression constructs included pMT-Myc-Abl (Xiong *et al.* 2009) Eya B isoform complementary DNA (cDNA) cloned into the gateway pAFW vector; Hop, Stat92E, Socs36E, and Socs44A cDNA cloned into the gateway pAHW vector; and SOCS mutants "QuikChanged" from pAHW-SOCS^{WT} plasmids. Oligos used were as follows: (1) Socs36E$^{\Delta NT}$, 5′-GGTACCAACACCATG AGCAGC TTCTACTGGGGC-3′ and 5′-GCCCCAGTAGAAGCTGCTCATG GTGTTGGTA CC-3′; (2) Socs36E$^{\Delta SH2}$, 5′-CTCGAGAAGATCAC GAACAGCGGTCACAAGTTCAG-3′ and 5′-CTGAACTTGTGAC CGCTGTTCGTGATCTTCTCGAG-3′; (3) Socs36E$^{SH2*\ (R500K)}$, 5′-GGCACGTTCCTGCTGAAAGACTCCGCCCAGGAGG-3′ and 5′-CCTCCTGGGCGG AGTCTTTCAGCAGGAACGTGCC-3′; (4) Socs36E$^{\Delta SB}$, 5′-CTGCACAGAAGGCAGACCT AGGAATTCGCG GCCGCA-3′ and 5′-TGCGGCCGCGAATTCCTAGGTCTGCCTTC TG TGCA G-3′; (5) Socs44A$^{\Delta NT}$, 5′-AACACCATGTACTGG GGTGAG-3′ and 5′-CTCACCCC AGTACATGGTGTT-3′; (6) Socs44A$^{\Delta SH2}$, 5′-AACCAAGTGTGGATCTTGCACCGC-3′ and 5′-G CGGTGCAAGATCCACACTTGGTT-3′; (7) Socs44A$^{SH2*\ (R214K)}$, 5′-TTTCTAGTC AAAGACTCGGAA-3′ and 5′-TTCCGAGTCTTT GACTAGAAA-3′; and (8) Socs44A$^{\Delta SB}$, 5′-CGGTACTCCAACTA GCTCGAG-3′ and 5′-CTCGAGCTAGTTGGAGTACCG-3′. For transfections containing Abl or Hop, cells were treated with 100 μM pervanadate and 200 μM H_2O_2 prior to fixation or lysis. Co-immunoprecipitation assays were performed by lysing cells in lysis buffer (50 mM Hepes, 150 mM NaCl, 1 mM EDTA, 0.5 mM EGTA, 0.9 M glycerol) supplemented with protease inhibitors (Roche), 0.5 mM DTT, and 0.1% Triton X-100, incubating the cell lysate with anti-Flag agarose beads (Sigma-Aldrich) overnight at 4°, washing three times with lysis buffer, and resolving the proteins on 8% SDS-PAGE gels. Proteins were

visualized by immunoblotting, using either mouse or rabbit anti-Flag (1:1000; Sigma-Aldrich) and rabbit or mouse anti-HA (1:1000; Rockland or 12CA5 University of Chicago Frank W. Fitch Monoclonal Antibody Facility, respectively) and secondary antibodies (1:2000; Li-COR Biosciences).

Eye imaginal discs and brains were dissected from prepupal third instar larvae and stained as previously described (Xiong *et al.* 2009) with rabbit anti-β-gal (1:20,000; Promega, Madison, WI). Transfected S2 cells were settled onto poly-L-lysine-treated slides, fixed with 4% paraformaldehyde for 10 min, and stained with anti-Flag and anti-HA as described above, followed by secondary antibodies (1:2000; Jackson ImmunoResearch). Samples were mounted with N-propyl-gallate solution in 90% glycerol.

Images were taken using a Zeiss LSM 510 confocal microscope. All axon images were taken at 0.5- to 1.5-μm steps for the entire depth of the brain and then projected maximally in ImageJ. All single cell images are single scans through the middle of the cell. Unless otherwise stated, statistical *P*-values were calculated by performing Student's *t*-test between control crosses with no RNAi transgene and the cross of interest. * *P*-value <0.05, ** *P*-value < 0.01, *** *P*-value < 0.001.

Fly strains and expression constructs are available upon request.

Data availability

The authors state that all data necessary for confirming the conclusions presented in the article are represented fully within the article.

Results and Discussion

A genetic screen for SH2/PTB family genes that synergize with eya during photoreceptor axon targeting

We previously showed that Eya shuttles between the nucleus and cytoplasm and that Abl-mediated tyrosine phosphorylation (pY) can sequester it in the cytoplasm (Xiong *et al.* 2009). These observations led us to hypothesize that pY–Eya might be recruited to cytoplasmic signaling complexes through interactions with Src homology 2 (SH2) or phosphotyrosine binding (PTB) domain-containing proteins. To test this idea, we leveraged our prior demonstration of genetic synergy between *eya* and *abl* during axon guidance (Xiong *et al.* 2009) to design an RNAi-based genetic interaction screen aimed at identifying SH2/PTB factors relevant to Eya function in differentiating photoreceptors.

Our prior work showed that in viable hypomorphic *eya* mutants, photoreceptor axons fasciculate aberrantly and frequently overshoot the lamina (Xiong *et al.* 2009). MARCM clones ruled out the possibility that these phenotypes stemmed from defects in the target layers of the brain, and *GMR–Gal4*-driven *eya* knockdown further confirmed its requirement in the photoreceptors (Xiong *et al.* 2009). Although the $GMR > Eya^{RNAi}$ mistargeting phenotype was modifiable, as evidenced by its enhancement upon *abl* knockdown (Xiong *et al.* 2009), we opted against using it as the primary background for our screen. Briefly, because we predicted positive genetic interactions between *eya* and relevant SH2/PTB genes, and therefore enhancement of the $GMR > Eya^{RNAi}$ phenotype, we were concerned that the difficulty in distinguishing a relevant enhancement from a nonspecific additive interaction would lead to a high false positive rate.

As an alternative, we explored the suitability of an *eya* overexpression phenotype for the screen. Using the membrane marker Ro-lacZ^{tau} (RTL) to label photoreceptors R2–R5 (Garrity *et al.* 1999), we quantified the average number of axon bundles that mistarget past the lamina to the medulla in $GMR\text{-}Gal4 > UAS\text{–}Eya^{WT}$ animals as 25.7 ± 6.1 (mean ± SD), a significant increase over the driver-alone baseline of 8.1 ± 2.2 (Figure 1, B *vs.* A and D) (Xiong *et al.* 2009). Reducing endogenous *eya* dosage with heterozygosity strongly suppressed the mistargeting (9.2 ± 4.4), confirming that the $GMR > Eya^{WT}$ phenotype resulted from increased Eya activity rather than from a dominant negative effect of *eya* overexpression (Figure 1, C and D).

Although the similarity between *eya* loss- and gain-of-function phenotypes may seem surprising, there is precedent for biological processes, including photoreceptor axon guidance, being sensitive to precisely balanced gene dosage such that both loss and gain produce similar phenotypes. For example, analogous to our observations with *eya*, either increased or decreased activity of the p21-activated kinase *Pak* (Hing *et al.* 1999) or of the transcription factor *hindsight* (Oliva and Sierralta 2010) causes photoreceptor axon mistargeting. It is also important to note that our system of counting the number of RTL-labeled axons that overshoot their laminar target, although highly effective as a first-pass quantification of a phenotype or interaction, ignores qualitative differences. For example, *eya* knockdown tends to produce thicker fascicles and greater disruptions to the lamina plexus than *eya* overexpression (Figure 1B, Supplemental Material, Figure S1) (Xiong *et al.* 2009). Future detailed mechanistic studies will be required to understand the requirement for balanced Eya levels in photoreceptor axon guidance, and the *eya* interactors identified in our screen should provide useful tools in that endeavor.

Given the general caveats associated with overexpression, it was critical to confirm the $GMR > Eya^{WT}$ mistargeting phenotype could be appropriately modified by a verified *eya* interacting gene. Building on our prior work (Xiong *et al.* 2009), we showed that reduced *abl* dose, either by heterozygosity or by expression of a weak $UAS\text{–}Abl^{RNAi}$ transgene that on its own did not produce targeting defects, dominantly suppressed $GMR > Eya^{WT}$ (13.4 ± 3.5 and 13.5 ± 5.4, respectively; Figure 1D shows data for Abl^{RNAi}). Thus reduced *abl* dominantly enhances *eya* loss-of-function and dominantly suppresses *eya* gain-of-function-induced axon mistargeting. We conclude that despite both overexpression and knockdown of *eya* causing axons to overshoot the lamina, these genetic backgrounds produce genetically distinct and biologically informative phenotypes and interactions.

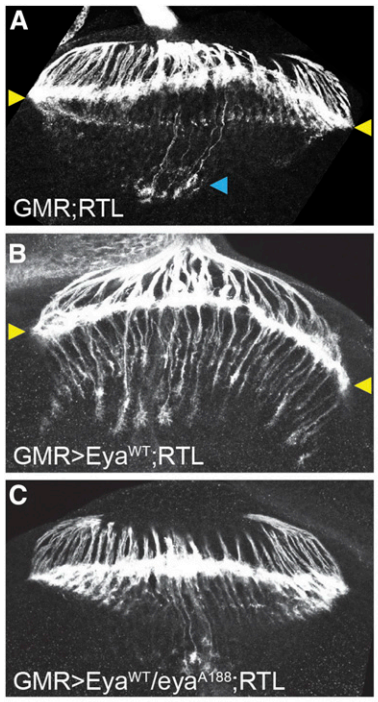

D

	w^{1118}	*eya/+*	abl^{RNAi}	Eya^{WT} Line 2
GMR-Gal4	8.0 ± 2.3 (50)	not tested	6.5 ± 2.8 (12)	24.0 ± 5.4 (21)
GMR>Eya^{WT} Line 1	25.7 ± 6.1 (11)	9.2 ± 4.4 (10)	13.5 ± 5.4 (22)	30.3 ± 4.1 (17)
GMR>Myr-Eya	18.9 ± 5.0 (65)	11.1 ± 4.3 (34)	8.7 ± 4.7 (31)	not tested
GMR>NLS-Eya	26.6 ± 4.9 (64)	11.6 ± 4.7 (7)	22.9 ± 4.3 (20)	not tested

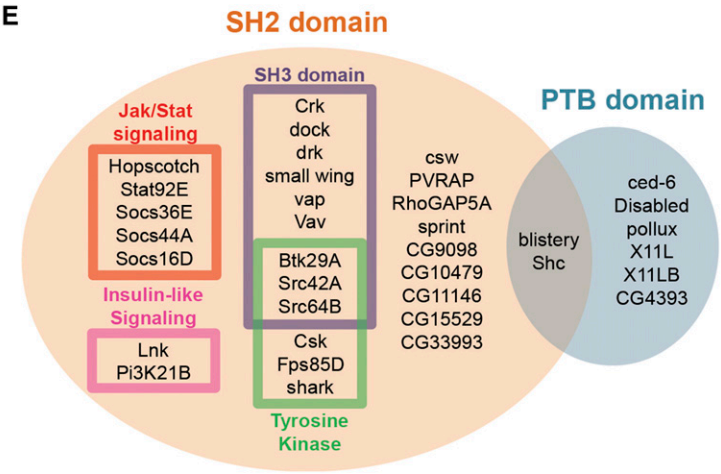

Figure 1 Eya overexpression axon targeting phenotypes provide dose-sensitive, suppressible genetic backgrounds. (A–C) The Ro-lacZ^{tau} (RTL) marker labels R2–R5 and is visualized by staining for β-galactosidase in third instar larval brains. (A) Wild-type RTL pattern shows most R2–R5 axons terminate correctly at the lamina, whose edges are marked by yellow arrowheads; a few axon bundles overshoot to the medulla, blue arrowhead. (B) *eya* overexpression causes many photoreceptor axon bundles to overshoot the lamina, marked by yellow arrowheads. (C) *eya* heterozygosity suppresses *eya* overexpression defects. (D) Quantification of genetic interaction tests, demonstrating *eya* overexpression phenotypes are dose sensitive and suppressible. *N* values are shown in parentheses. (E) Thirty-six SH2/PTB domain-containing genes in *Drosophila*, grouped into known categories of signaling, that were targeted in our RNAi-based genetic screen.

We also tested sensitivity of the *GMR* > Eya^{WT} background to enhancement by coexpressing a second *UAS–*Eya^{WT} transgene that had a comparably strong phenotype as the first (24.0 ± 5.4), but found only a modest increase to 30.3 ± 4.1 mistargeted axon bundles per brain. Thus the overexpression phenotype was dose sensitive toward suppressive interactions, but was not easily enhanced (Figure 1D). Because we predicted that reducing the dosage of an SH2/PTB-containing factor relevant to cytoplasmic Eya functions would suppress rather than enhance, the *GMR* > Eya^{WT} background seemed ideal for the screen.

We screened a collection of 63 RNAi transgenes that targeted 36 SH2/PTB family genes for their ability to suppress the *GMR* > Eya^{WT} axon targeting phenotype (Figure 1E). This panel included two independent RNAi transgenes per gene whenever possible to minimize the likelihood of false positives from off-target effects and false negatives from insufficient knockdown. Our use of *GMR–Gal4* restricted knockdown to retinal cells posterior to the morphogenetic furrow, thereby bypassing any earlier requirements for the SH2/PTB genes to be tested. The screen was performed blind as to SH2/PTB gene identity, and ~10–20 third larval instar eye–brain complexes were dissected, stained, and scored for each interaction test.

To prioritize further study, suppressors were binned into strong, moderate, or mild interest groups based on *P*-value. A total of 11 strong ($P < 0.001$), 6 moderate ($P < 0.01$), and 10 mild ($P < 0.05$) hits were recovered, identifying 21 potential *eya* interacting genes (Table 1 shows genes with one strong or moderate hit; full screen results are in Table S1). The rather high hit rate from the primary screen may reflect extensive connectivity between phosphotyrosine signaling modules (Koytiger *et al.* 2013). Inclusion of *dab*, a positive factor in the Abl signaling network (Song *et al.* 2010), in this initial list provided proof of principle for the screen by highlighting the importance of *eya–abl* interactions to axon guidance and thereby further validating the biological relevance of the *eya* overexpression phenotype. To narrow the scope of the follow-up experiments to a technically manageable level, we focused only on the strong and moderate suppressors, with one exception, *Stat92E*.

Genetic triage highlights potential links between Eya and both the Jak/Stat signaling pathway and nonreceptor tyrosine kinases

Three secondary genetic tests were used to verify these hits as *bona fide* genetic interactors and to determine which genes may be relevant to cytoplasmic Eya function. First, we asked whether lines that suppressed *GMR* > Eya^{WT} conversely enhanced *eya* loss-of-function axon targeting phenotypes (Table 1). All but three genes (*CG15529*, *plx*, and *vap*) enhanced *GMR* > Eya^{RNAi}, while *shark* yielded mixed results, as one *shark* RNAi line enhanced and the other suppressed. Next, we used membrane-tethered myristoylated Eya (Myr–Eya) and nuclearly localized Eya (NLS–Eya) (Xiong *et al.* 2009) to distinguish

Table 1 Short list of candidate Eya-interacting SH2/PTB genes after primary and secondary genetic interaction tests

RNAi element	GMR > Eya^{WT};RTL	GMR > Eya^{RNAi};RTL	GMR > Myr-Eya^{WT};RTL	GMR > NLS-Eya^{WT};RTL
None (w^{1118})	25.7 ± 6.1	18.8 ± 2.5	18.9 ± 5.0	26.6 ± 4.9
$Stat92E^{43866}$	19.8 ± 2.6* ↓	21.1 ± 3.3* ↑	13.6 ± 4.5** ↓	31.6 ± 4.9** ↑
$Stat92E^{106980}$	19.3 ± 6.1* ↓	25.0 ± 3.7*** ↑	12.9 ± 4.8*** ↓	42.3 ± 7.3*** ↑
$Socs36E^{51821}$	22.3 ± 3.8			
$Socs36E^{52182}$	17.7 ± 4.4** ↓	22.0 ± 4.4* ↑	11.2 ± 4.1*** ↓	27.5 ± 7.6
$Socs44A^{33489}$	25.4 ± 3.8			
$Socs44A^{102764}$	14.3 ± 5.3*** ↓	21.0 ± 4.0* ↑	12.1 ± 7.3** ↓	40.7 ± 3.5*** ↑
hop^{40037}	22.4 ± 4.8			
hop^{102830}	16.6 ± 6.8*** ↓	23.2 ± 5.1* ↑	14.3 ± 6.2* ↓	39.8 ± 6.6*** ↑
$Src42A^{100708}$	12.7 ± 4.3*** ↓	21.3 ± 4.0* ↑	10.6 ± 5.1*** ↓	36.1 ± 5.4*** ↑
$Src64B^{35252}$	15.5 ± 2.9*** ↓	22.8 ± 3.8*** ↑	9.8 ± 3.2*** ↓	20.2 ± 4.9*** ↓
Csk^{32877}	16.7 ± 4.0*** ↓	24.5 ± 4.7*** ↑	12.1 ± 5.2*** ↓	41.0 ± 6.5** ↑
$shark^{25304}$	17.2 ± 4.7*** ↓	23.3 ± 2.3*** ↑	10.3 ± 3.8*** ↓	36.8 ± 4.5*** ↑
$shark^{105706}$	18.4 ± 3.1** ↓	16.1 ± 3.4*** ↓		
Lnk^{32892}	22.6 ± 3.3			
Lnk^{103646}	13.4 ± 6.5*** ↓	23.3 ± 4.6* ↑	12.6 ± 5.3*** ↓	45.3 ± 6.0*** ↑
vap^{44638}	20.2 ± 5.7* ↓			
vap^{107341}	17.9 ± 5.9** ↓	17.1 ± 2.9* ↓		
csw^{21756}	18.6 ± 4.7** ↓	24.5 ± 3.4*** ↑	19.9 ± 6.2	20.9 ± 4.4*** ↓
csw^{21757}	22.7 ± 2.9			
$CG15529^{50228}$	21.8 ± 7.7			
$CG15529^{100438}$	17.9 ± 2.8** ↓	18.8 ± 2.6		
Dab^{13005}	18.1 ± 6.7** ↓	23.6 ± 2.9*** ↑	14.8 ± 3.5** ↓	13.7 ± 3.6*** ↓
Dab^{14008}	13.0 ± 4.3*** ↓	24.0 ± 2.7*** ↑	11.8 ± 2.7*** ↓	25.7 ± 5.0
plx^{27335}	6.54 ± 3.1*** ↓	19.8 ± 3.3		
plx^{106969}	26.6 ± 4.5			
$X11L^{27479}$	13.5 ± 4.4*** ↓	24.7 ± 5.1* ↑	11.1 ± 4.4*** ↓	34.8 ± 4.6*** ↑
$X11L\beta^{8309}$	10.4 ± 5.1*** ↓	21.8 ± 3.9* ↑	19.8 ± 6.0	33.4 ± 4.2*** ↑
$X11L\beta^{14872}$	27.4 ± 5.8			

A short list of RNAi lines identified in the primary screen as suppressors were crossed to *GMR > Eya^{RNAi};RTL*, *GMR > Myr-Eya^{WT};RTL*, and *GMR > NLS-Eya^{WT};RTL* backgrounds as secondary tests. Numbers shown are averages of overshooting axons per brain with SD. Superscripted numbers for each RNAi element indicate the VDRC stock line used. Solid down arrows mark significant suppressive interactions; open up arrows mark enhancement. Full table of results for all RNAi lines screened along with *N* values can be found in Table S1. * *P*-value <0.05, ** *P*-value <0.01, *** *P*-value <0.001.

interactions specific to Eya's cytoplasmic and nuclear functions, respectively. *GMR–Gal4*-driven expression of both *Myr–Eya* and *NLS–Eya* produce axon guidance defects that can be suppressed by *eya* heterozygosity (Figure 1D), indicating gain-of-function effects. However, we hypothesized that *Myr–Eya* and *NLS–Eya* perturb axon targeting via distinct mechanisms given their restricted subcellular localizations. Consistent with this idea, *abl* knockdown suppressed the axon mistargeting phenotypes associated with *Myr–Eya* but not *NLS–Eya* (Figure 1D). Of the candidate lines tested, all except *csw* and *X11Lβ* significantly suppressed *GMR > Myr–Eya* mistargeting defects (Table 1). When tested against *GMR > NLS–Eya*, only *Src64B* and *csw* suppressed, while the remaining 10 lines enhanced. Because relevant interactions with *eya* gain-of-function phenotypes should manifest as suppression, we suspected the enhancement of *GMR > NLS–Eya* reflected additive effects rather than real interactions. Consistent with this prediction, *GMR–Gal4* knockdown of these SH2/PTB genes produced significant targeting defects (Figure 2A). In sum, the results of our secondary screens whittled the number of candidates to 10 genes: *Csk*, *hop*, *Lnk*, *shark*, *Socs36E*, *Socs44A*, *Src42A*, *Src64B*, *Stat92E*, and *X11L*. Among these, *Src64B* was unique in its potential to influence both cytoplasmic and nuclear Eya functions.

Two groups of genes were notably enriched in this short list: the Jak/Stat pathway (*hop*, *Stat92E*, *Socs36E*, and *Socs44A*) and nonreceptor tyrosine kinases (*Csk*, *hop*, *shark*, *Src42A*, and *Src64B*). In the follow-up studies described below, we focused on uncovering the mechanistic links that may underlie the Jak/Stat signature. Two reasons drove this decision. First, because the Jak/Stat pathway had not been previously implicated in axon guidance in any system, discovery of a novel context for Jak/Stat signaling in neuronal development had the potential for the broadest impact. Second, with the exception of *Stat92E*, the interactions that produced our 10-gene short list were based on a single RNAi transgene, either because only one line was available (*Csk*, *Src42A*, *Src64B*, and *X11L*) or because only one of the two lines tested showed interaction in the primary (*hop*, *Lnk*, *Socs36E*, and *Socs44A*) or secondary (*shark*) screens (Table 1, Table S1). Independent identification of four different Jak/Stat pathway members provided collective validation, and so mitigated the risk of pursuing spurious off-target effects of single hits. In the future, comparison of target gene messenger RNA levels between pairs of lines and addition of Dicer2 to the line that did not interact could be performed to determine whether such discrepancies reflect false positives due to off-target effects or false negatives due to either poor RNAi efficiency or additive interactions. We consider the latter to be the most likely explanation, given that our screen required suppression of *GMR > Eya^{WT}* by RNAi knockdowns that on their own often produced strong mistargeting

A

RNAi element	GMR;RTL	n
none (w^{1118})	8.0 ± 2.3	50
hop^{40037}	15.3 ± 2.1***	12
hop^{102830}	22.3 ± 3.6***	18
$Stat^{43866}$	19.7 ± 4.5***	15
$Stat^{106980}$	18.8 ± 3.0***	7
$Socs36E^{51821}$	17.1 ± 2.8***	18
$Socs36E^{52182}$	16.7 ± 3.1***	9
$Socs44A^{33489}$	9.5 ± 3.6	13
$Socs44A^{102764}$	11.9 ± 2.8**	16
$Src42A^{100708}$	18.0 ± 1.6***	8
$Src64B^{35252}$	18.1 ± 3.7***	17
Csk^{32877}	17.4 ± 3.5***	8
$shark^{25304}$	19.0 ± 1.9***	6
$shark^{105706}$	21.5 ± 1.1***	8
Lnk^{103646}	23.3 ± 1.3***	7
$x11L^{27479}$	19.7 ± 2.5***	7

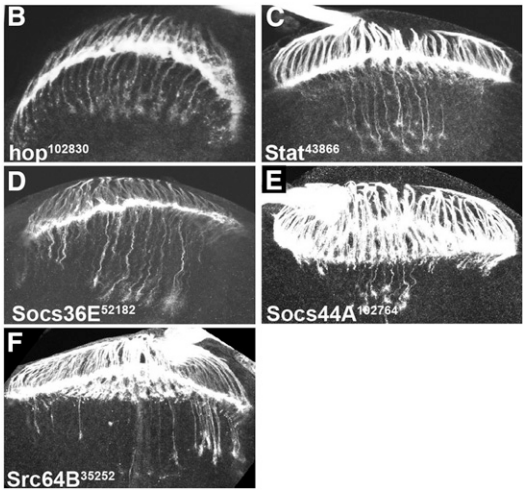

Figure 2 Eya-interacting SH2/PTB genes are required for photoreceptor axon guidance. (A) Quantification of axon mistargeting phenotypes resulting from RNAi knockdown of 10 SH2/PTB genes from Table 1. The RNAi lines indicated were crossed to *GMR;RTL*. Superscripted numbers indicate the VDRC stock used. Numbers shown are averages of overshooting axons per brain with SD. * *P*-value <0.05, ** *P*-value < 0.01, *** *P*-value < 0.001. *N* values are shown on the right. (B–F) Representative brains of the indicated genotype stained with β-galactosidase.

defects (Figure 2A). Thus a "hit" in the primary screen often reflects not only suppression of *eya* overexpression phenotypes by SH2/PTB knockdown, but also mutual suppression of SH2/PTB knockdown phenotypes by increased *eya* dose. In cases where the additive effects were sufficiently strong as to mask such mutual suppression, inconsistent results between independent lines would be expected.

The second category of interactors, the nonreceptor tyrosine kinases, underscores the importance of phosphotyrosine-based signaling for photoreceptor axon targeting. Previous work hinted at this, as a number of tyrosine phosphatases were found to be critical for regulating axon targeting (Garrity *et al.* 1999; Schindelholz *et al.* 2001; Jeon *et al.* 2008). Our results identify a set of candidate tyrosine kinases that could provide the opposing catalytic activity. The remaining two genes on the short list, *Lnk* and *X11L*, encode adapter proteins. X11L has been implicated in amyloid precursor protein (APP) regulation in both *Drosophila* and mammalian cells (Hase *et al.* 2002; Gross *et al.* 2008), with no reported connections to either Jak/Stat or tyrosine kinase signaling. *Lnk* negatively feeds back on Jak/Stat signaling in mammalian cells, although in *Drosophila* it has been studied as a positive regulator of insulin/insulin-like growth factor signaling (Werz *et al.* 2009; Oh *et al.* 2010; Slack *et al.* 2010; Almudi *et al.* 2013). The Jak/Stat ligands unpaired (Upd) 2 and 3 influence insulin signaling in *Drosophila* (Rajan and Perrimon 2012; Woodcock *et al.* 2015), thus potentially implicating Lnk in Jak/Stat signaling in flies.

Jak/Stat signaling is necessary for photoreceptor axon guidance

Jak/Stat signaling in *Drosophila* is transduced via three ligands, Upd1–3, one receptor, Dome, one Janus kinase (JAK), Hopscotch (Hop), and one signal transducer and activator of transcription (STAT), Stat92E (Stat). Signaling can be attenuated by a variety of negative regulators, including the suppressor of cytokine signaling (SOCS) proteins encoded by *Socs36E* and *Socs44A* (Rawlings *et al.* 2004a,b; Arbouzova and Zeidler 2006). Jak/Stat signaling directs a diverse spectrum of developmental events including cell migration, proliferation, patterning, and morphogenesis (reviewed in Arbouzova and Zeidler 2006 and Li 2008). During eye development, the pathway promotes growth of the early eye field, contributes to initiation and movement of the morphogenetic furrow and to regional eye specification, transduces information from the dorsal–ventral axis to direct ommatidial rotation, and regulates specification and maintenance of the optic lobe neuroepithelium (Luo *et al.* 1999; Zeidler *et al.* 1999; Chao *et al.* 2004; Tsai and Sun 2004; Ekas *et al.* 2006; Gutierrez-Aviño *et al.* 2009; Ngo *et al.* 2010; Wang *et al.* 2011).

Identification of *hop*, *Stat92E*, *Socs36E*, and *Socs44A* in our genetic screen (Table 1) and finding that *GMR*-driven knockdown of these genes produces axon mistargeting phenotypes (Figure 2, A–E) suggested that the Jak/Stat pathway is also active in postmitotic photoreceptors. In support of this, expression of the 10xStat–eGFP pathway activity reporter suggests that early expression of the ligand, *upd*, which is absent by the third instar, enables sustained Jak/Stat signaling in the photoreceptors at the time they are sending out their axons (Bach *et al.* 2007). As predicted, *GMR–Gal4*-driven knockdown of the receptor *dome*, but not of the *upd* ligands, produced significant mistargeting defects (Figure 3, A–C).

To confirm further the requirement for Jak/Stat signaling in photoreceptor axon guidance, we generated MARCM clones of a *Stat92E* null allele, $stat^{85c9}$. Axons originating in photoreceptors that lacked *Stat92E* overshot the lamina into wild-type brain tissue (Figure 3D), while clones within the brain did not cause mistargeting of wild-type photoreceptors (data not shown). This demonstrates that correct axon targeting requires *Stat92E* in the photoreceptors. The result also eliminates the possibility that RNAi-induced phenotypes resulted from either leaky *GMR–Gal4* expression in the brain (Li *et al.* 2012) or off-target effects. Together, our results indicate a cell autonomous role for Jak/Stat signaling in postmitotic photoreceptors that directs axon projections to the correct layers of the brain.

One apparent inconsistency between this conclusion and our genetic screen results is that SOCS factors typically antagonize Jak/Stat signaling (Chen *et al.* 2000; Callus and

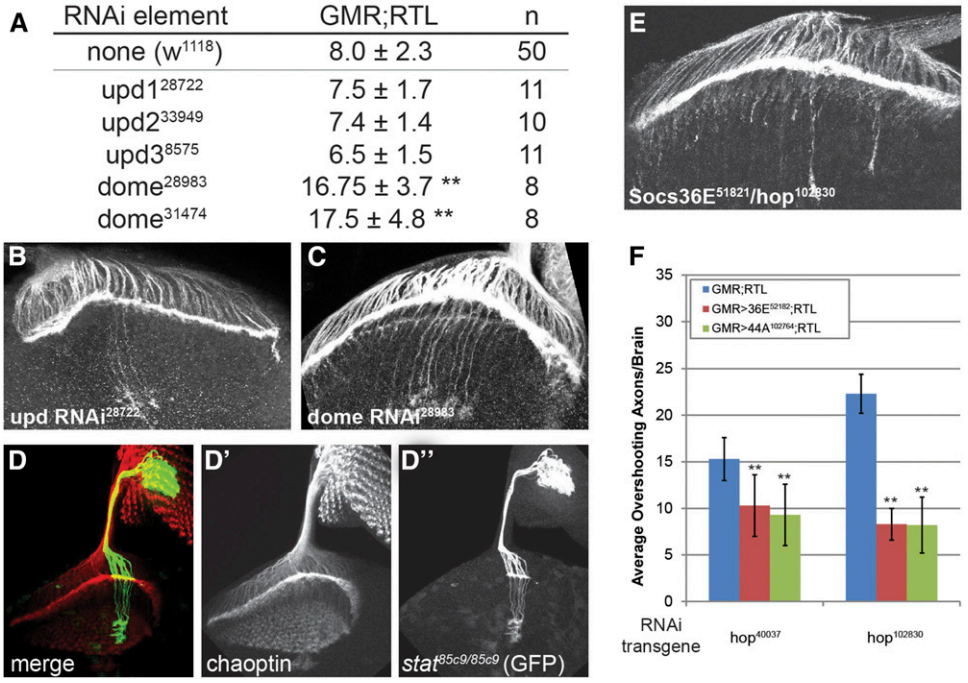

Figure 3 Jak/Stat signaling is required cell autonomously in photoreceptors for axon targeting. (A) Quantification of axon mistargeting phenotypes, resulting from RNAi knockdown of *upd* and *dome*. The RNAi lines indicated were crossed to *GMR;RTL*. Superscripted numbers indicate the Bloomington stock used. Numbers shown are averages of overshooting axons per brain with SD. * *P*-value <0.05, ** *P*-value < 0.01, *** *P*-value < 0.001. *N* values are shown to the right. (B and C) Representative brains of the indicated genotype stained with β-galactosidase. (B) *upd* knockdown does not perturb axon targeting. (C) Knockdown of *dome* leads to significant overshooting of the lamina. (D) GFP+ (green) MARCM clone showing that the axons of *Stat92E* null photoreceptors overshoot the lamina. Chaoptin staining (red) marks all photoreceptors in the eye disc (top right) and highlights their axonal projections through the optic stalk and into the brain. (E) Representative brain stained with β-galactosidase, showing that *Socs36E* knockdown suppresses the axon mistargeting phenotypes of *GMR > hop*^{RNAi} (compare to Figure 2B) (F) Quantification and statistics of axon overshooting phenotypes in double knockdown interaction assays show that *Socs* genes function as Jak/Stat pathway antagonists. *GMR;RTL* (blue), *GMR > Socs36E*^{RNAi}*;RTL* (red), and *GMR > Socs44A*^{RNAi}*;RTL* (green) were crossed to the *hop*^{RNAi} line indicated on the *x*-axis. *N* values per experiment from left to right are 10, 7, 10, 13, 13, and 14. *P*-values were calculated by performing Student's *t*-test between the experimental cross and driver-alone control (*i.e.*, red/green *vs.* blue). * *P*-value <0.05, ** *P*-value <0.01, *** *P*-value <0.001. Superscripted numbers refer to VDRC RNAi line.

Mathey-Prevot 2002; Rawlings *et al.* 2004b) yet knockdown of *Socs*, *hop*, or *Stat92E* all suppressed *GMR > Eya*^{WT}. Since axon targeting is a novel context for Jak/Stat signaling, one possibility is that the SOCS factors do not antagonize the pathway in postmitotic photoreceptors as they do in other situations (Callus and Mathey-Prevot 2002; Rawlings *et al.* 2004b). Arguing against this, knockdown of either *Socs36E* or *Socs44A* suppressed the *GMR > hop*^{RNAi} mistargeting phenotypes (Figure 3, E and F). In addition to their roles as negative regulators of Jak/Stat signaling, SOCS factors also influence a variety of growth factor signaling cascades (De Sepulveda *et al.* 1999; Chen *et al.* 2000; Bayle *et al.* 2004; Rawlings *et al.* 2004b; Kazi *et al.* 2012; Trengove and Ward 2013). Thus the *eya–Socs* synergy observed in our screen could reflect interactions relevant to those other pathways. Mechanistically, although SOCS proteins belong to the family of Cullin–Ring E3 ubiquitin ligases (reviewed in Piessevaux *et al.* 2008), a model in which they target Eya for degradation seemed unlikely because the predicted increase in Eya levels upon *Socs* knockdown should enhance, rather than suppress, *GMR > Eya*^{WT} phenotypes. Consistent with such reasoning, *Socs* knockdown did not alter Eya protein levels in the *GMR > Eya*^{WT} background (data not shown).

Given the sensitivity of photoreceptor axon targeting to both loss and overexpression of *eya* (Figure 1, Table 1, Figure S1), we asked whether the same might hold true for *hop*, *Stat92E*, *Socs36E*, and *Socs44A*. *GMR–Gal4*-driven overexpression of *hop* was lethal prior to the third instar, and *Stat92E* overexpression did not produce targeting defects (data not shown and Figure 4, A and C). *Stat92E* overexpression also did not modify *GMR > Eya*^{RNAi} (Figure 4, B and F), suggesting endogenous signaling is limited and insufficient to activate the extra Stat protein. Consistent with this interpretation, previous reports have shown that although *UAS–Stat* can rescue *Stat92E* null phenotypes, its overexpression in an otherwise wild-type background does not perturb eye development (Ekas *et al.* 2006).

In contrast, *GMR–Gal4*-driven overexpression of either *Socs36E* or *Socs44A* significantly perturbed axon targeting (Figure 4, A, D, and E). We took advantage of this result to validate independently the *Socs–eya* synergy predicted by our genetic screen interactions. Just as *Socs* knockdown suppressed *eya* overexpression phenotypes (Table 1), *Socs* overexpression suppressed *eya* knockdown phenotypes (Figure 4, B, G, and H). Thus cooperative *eya–Socs* interactions appear integral to photoreceptor axon targeting.

Eya co-immunoprecipitates and colocalizes with Socs44A via an SH2–pY-mediated interaction

Given that the impetus for our genetic screen was the possibility that SH2/PTB domains interact with pY–Eya, we next asked whether Eya could co-immunoprecipitate (CoIP) Jak/Stat proteins from lysates of *Drosophila* S2 cultured cells transiently transfected with epitope-tagged expression constructs. CoIPs were performed both with and without cotransfection of Abl. We found that Flag-tagged Eya can

A

UAS element	GMR;RTL	N
none (w^{1118})	8.0 ± 2.3	50
$Stat^{WT}$	8.1 ± 2.0	9
$Socs36E^{WT}$	30.8 ± 5.9***	9
$Socs44A^{WT}$	23.7 ± 4.0***	7

B

UAS element	GMR;RTL	N
Eya^{RNAi}	18.8 ± 2.5	33
Eya^{RNAi}, $Stat^{WT}$	19.3 ± 2.9	9
Eya^{RNAi}, $Socs36E^{WT}$	9.7 ± 2.4***,***	7
Eya^{RNAi}, $Socs44A^{WT}$	12.5 ± 3.5**,***	14

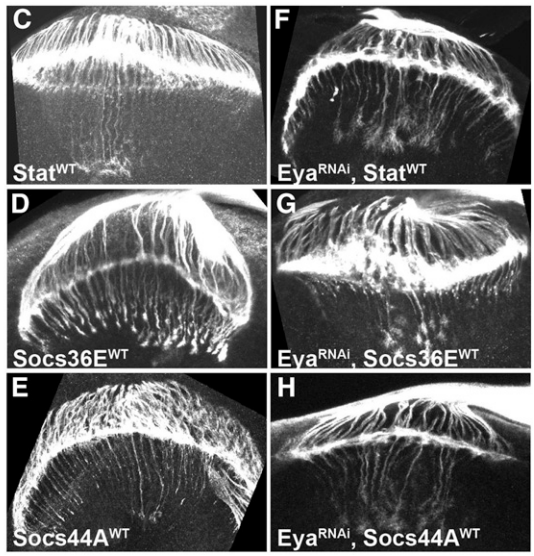

Figure 4 Eya and SOCS synergize in axon targeting. (A) Quantification of axon phenotypes resulting from overexpression of *Stat92E*, *Socs36E*, and *Socs44A*. (B) Quantification of axon phenotypes from genotypes in (A) in a *GMR* > Eya^{RNAi} background. (C–H) Representative images of the indicated genotypes stained with anti-β-galactosidase. *P*-values were calculated by performing Student's *t*-test between the experimental cross and the control of that group. In B, the first is relative to *GMR* > Eya^{RNAi} and the second is relative to *GMR* > $SOCS^{WT}$, revealing mutual suppression. * *P*-value <0.05, ** *P*-value <0.01, *** *P*-value <0.001.

CoIP HA-tagged Hop, Socs36E, and Socs44A, but not Stat, and that Abl improved Eya's CoIP of Socs36E and Socs44A, but not that of Hop or Stat (Figure 5, A–D). Abl stimulates Eya tyrosine phosphorylation and cytoplasmic accumulation (Xiong *et al.* 2009 and Figure 6, A *vs.* B, quantified in N) and thus should enhance SH2/PTB–pY–Eya interactions. Abl is expressed endogenously in S2 cells (Cherbas *et al.* 2011), and some tyrosine phosphorylation of Eya can be detected in cells transfected with Eya alone (Tootle *et al.* 2003), perhaps explaining the low levels of Socs36E and Socs44A CoIP detected when Abl was not supplied by cotransfection (Figure 5, C and D). The Abl independence of the Eya–Hop CoIP (Figure 5A) suggests that either Hop phosphorylates Eya at different tyrosine residues, or that pY–SH2 interactions do not drive the CoIP.

Because Abl increased Eya's CoIP with Socs36E and Socs44A, we focused on them as the top candidates for forming SH2–pY–Eya complexes. To test this, we generated three deletion mutants that removed either the N terminus (ΔNT), the SH2 domain (ΔSH2), or the Socs Box (ΔSB) and a point mutant (SH2*, $Socs36E^{R500K}$, or $Socs44A^{R214K}$) that compromises SH2 function in homologous mammalian SOCS proteins (Nicholson *et al.* 1999). Consistent with expectations, the Socs44A SH2 domain was required for CoIP, while the SH2* point mutant weakened the interaction (Figure 5F, Figure S2). Similar experiments with Socs36E did not identify any single domain as being required for CoIP (Figure 5E), suggesting that the Eya–Socs36E interaction is more complicated, either requiring multiple Socs36E domains to assemble the complex and/or additional proteins to bridge the interactions. Socs44A and Socs36E are both endogenously expressed in S2 cells (Callus and Mathey-Prevot 2002; Zhu *et al.* 2013) and can CoIP each other (Figure S3). Thus, Socs44A is an appealing candidate to bridge the Eya–Socs36E interaction, as its association with both proteins would confer the sensitivity to Abl seen in the Eya–Socs36E CoIPs (Figure 5C).

The pY–SH2-mediated CoIP of Eya and Socs44A predicted cytoplasmic colocalization. Our previous work has shown that Eya is predominantly nuclear but can be relocalized to the cytoplasm upon phosphorylation by Abl (Xiong *et al.* 2009 and Figure 6, A and B). Socs44A accumulated in the cytoplasm, with strong association to the plasma membrane (Figure 6, C and F–I; localization of Hop, Stat, and Socs36E is shown in Figure S4). In Eya–Socs44A cotransfected cells, we observed a subtle increase in the proportion of cells with cytoplasmic Eya, while Socs44A localization was not changed (Figure 6, F, G, and N). Occasionally, membrane-associated Eya puncta were observed and these tended to colocalize with $Socs44A^{+}$ spots (Figure 6G). The frequency of cells displaying these punctate structures dramatically increased when Abl was cotransfected (Figure 6, H, I, and O). Confirming the SH2 requirement for Eya recruitment, we did not observe Eya-containing puncta when $Socs44A^{\Delta SH2}$ was expressed (Figure 6, J, K, and O). To separate Abl's role in phosphorylating Eya from its role in recruiting Eya to the cytoplasm, we examined the response of Myr–Eya, which is constitutively targeted to the cytoplasmic membrane (Figure 6, D and E). Only when Abl was cotransfected did Socs44A promote Eya punctate localization (Figure 6, L, M, and O). We speculate that these puncta represent Eya–Socs44A complexes and that they are mediated by pY–SH2 interactions.

Concluding remarks

Our genetic screen was initially motivated by the idea that the cytoplasm was a likely site for Eya's phosphotyrosine phosphatase activity (Xiong *et al.* 2009), a model which was subsequently validated in mammals (El-Hashash *et al.* 2012). Recent work has shown that this catalytic function of Eya is dispensable for *Drosophila* development (Jin *et al.* 2013). What then might be the role of cytoplasmic Eya? One possibility is that Eya might act as a scaffolding factor that nucleates the formation of specific protein complexes in response to different upstream signals. Because our biochemical

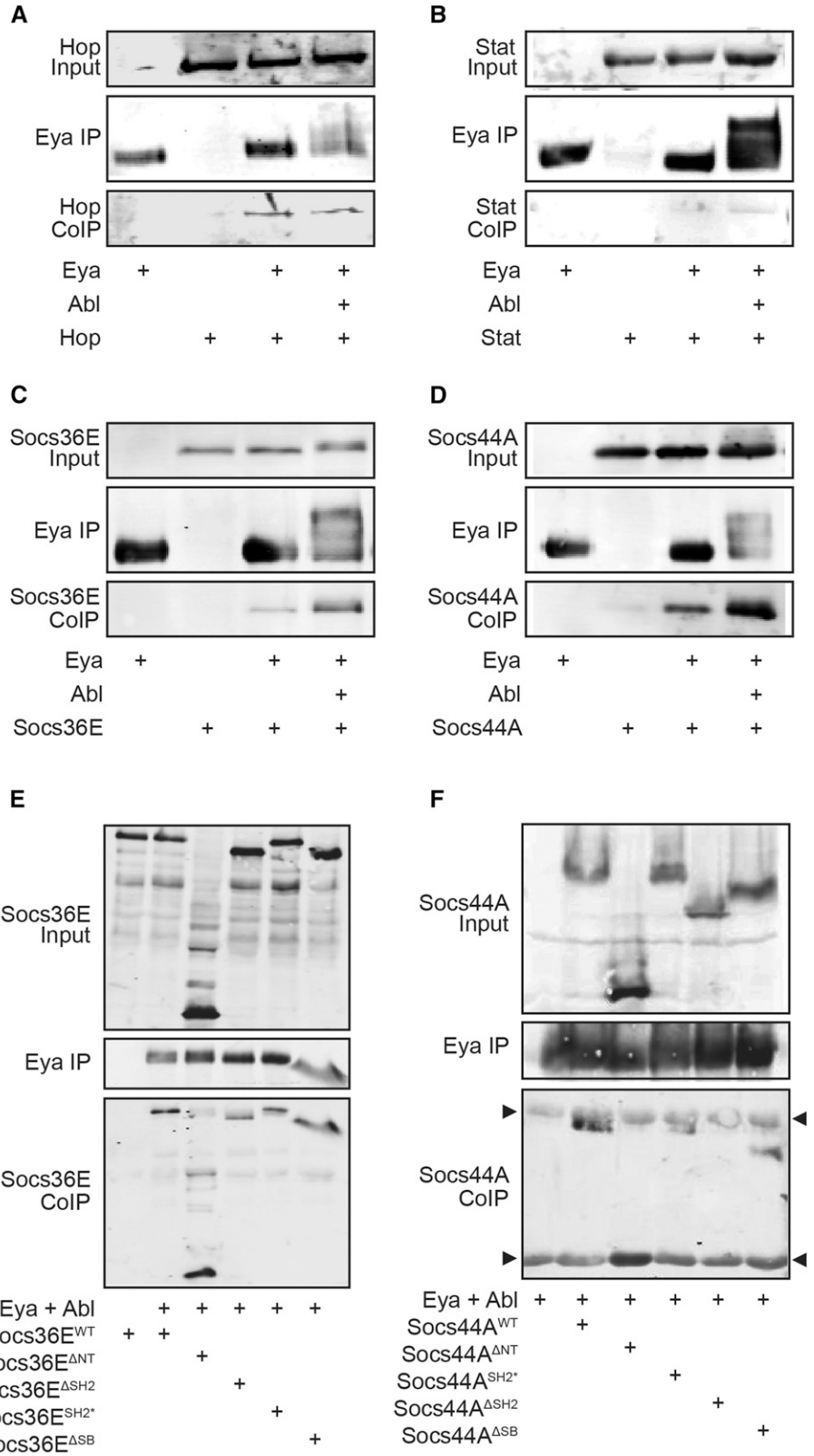

Figure 5 pY–SH2 dependence of Eya CoIP with Hop, Socs36E, and Socs44A. (A–F) Western blots showing CoIP results from transfected *Drosophila* S2 cells. Top panels, blotted with anti-HA, show input levels for the HA-tagged Jak/Stat pathway factor. Middle panels, blotted with anti-Flag, show IP of Flag–Eya. Bottom panels show CoIP of the HA-tagged Jak/Stat pathway protein. Key below indicates factors transfected in each experiment. (A–D) Eya CoIPs full-length Hop, Socs36E, and Socs44A but not Stat. Broad smeary band in lane 4, middle panels, reflects the extensive tyrosine phosphorylation of Eya that occurs in the presence of Abl (Xiong *et al.* 2009). (A) Flag–Eya CoIPs HA–Hop in the presence or absence of Abl. (B) Flag–Eya does not CoIP HA–Stat. (C and D) Flag–Eya CoIP of Socs36E (C) and Socs44A (D) is increased in the presence of Abl. (E and F) Eya–Socs44A but not Eya–Socs36E requires the SH2 domain of that SOCS factor. (E) Flag–Eya CoIPs all HA–Socs36E mutant constructs. (F) Flag–Eya CoIPs all HA–Socs44A deletion constructs except that lacking the SH2 domain. Black triangles mark IgG bands. Full-length Socs44A (lanes 2 and 4) runs below IgG heavy chain, while Socs44A$^{\Delta NT}$ runs coincident with IgG light chain (lane 3).

experiments relied on interactions between overexpressed proteins in cultured cells, it will be important to confirm the results using endogenous proteins from *Drosophila* tissues. Another possibility is that Eya might modulate the composition or function of such complexes via its phosphothreonine phosphatase activity. Eya's threonine phosphatase activity has been implicated in innate immunity in both mammals and *Drosophila*, and although substrates have not been identified,

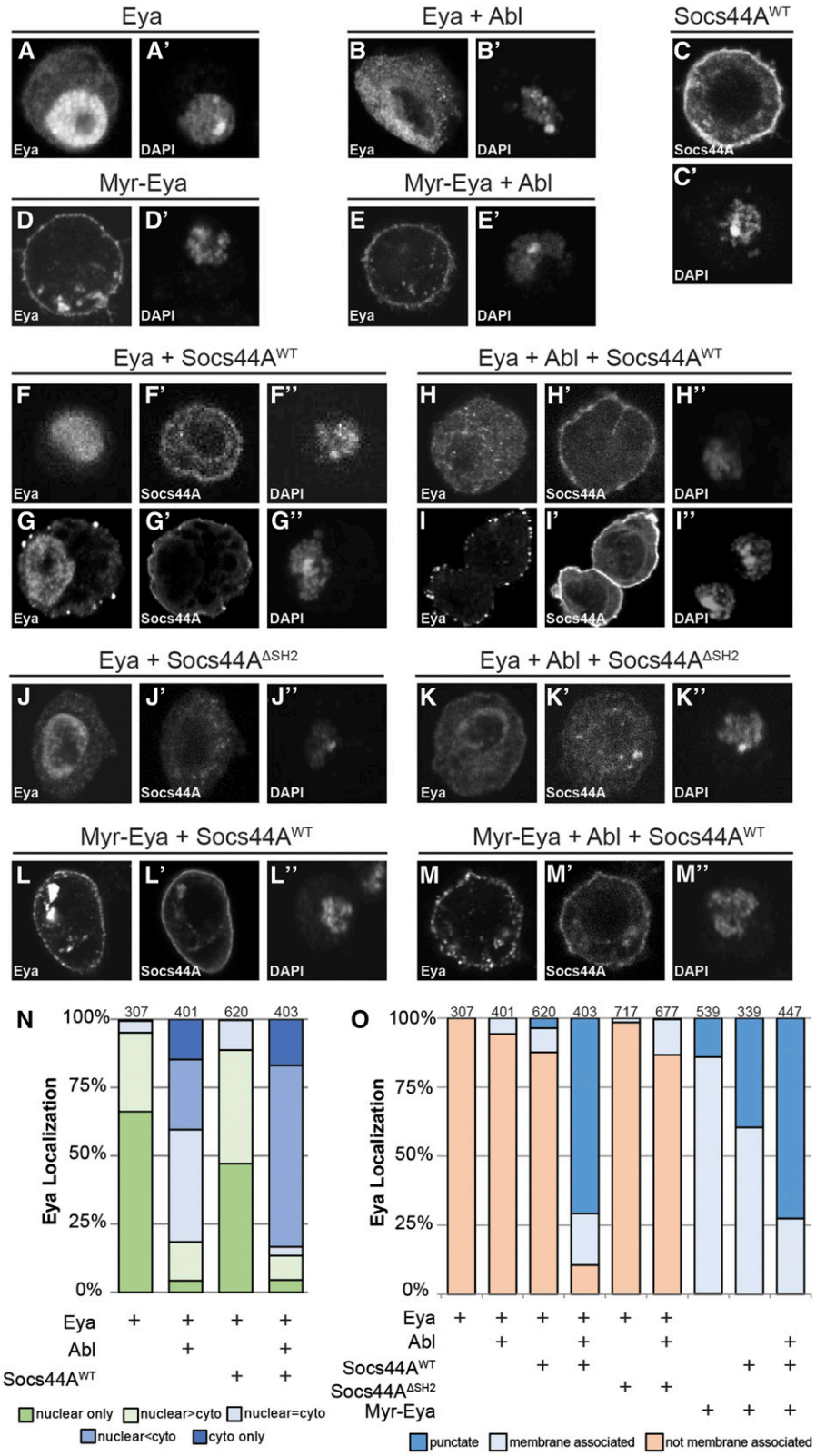

Figure 6 Eya localizes to cytoplasmic punctate structures when cotransfected with Abl and Socs44A. (A–M) Individual transfected S2 cells showing representative subcellular distribution of Flag–Eya and HA–Socs44A. Nuclei are marked with DAPI. (A) Flag–Eya is predominantly nuclear. (B) Cotransfection of Abl causes cytoplasmic redistribution of Flag–Eya. (C) Full-length HA–Socs44A appears cytoplasmic and membrane associated. (D) Myr–Flag–Eya is tightly membrane associated, with some punctate structures apparent. (E) Cotransfection of Abl does not alter Myr–Flag–Eya distribution. (F and G) Two representative cells showing that cotransfection of Socs44A does not induce a major redistribution of Eya (F), although in a small fraction of cells, bright membrane proximal punctate structures are seen (G). Socs44A appears more tightly membrane associated in cells in which Eya puncta form (G′), with reduced general cytoplasmic accumulation (compare to F′). (H and I) Two representative cells showing Eya cytoplasmic (H) and punctate (I) localization increases in response to cotransfection of Abl and Socs44A. In cells with Eya puncta, Socs44A tends to be strongly membrane associated (I′). (J and K) Redistribution of Eya to membrane-associated puncta requires the SH2 domain of Socs44A. Socs44A$^{\Delta SH2}$ localizes diffusely throughout the cytoplasm and is not strongly membrane associated (Figure S3L), and localization does not change with cotransfection of Eya (J) or Eya and Abl (K). (L) Socs44A only slightly increases the punctate distribution of Myr–Eya. (M) Cotransfection of Abl and Socs44A results in punctate Myr–Eya distribution in 75% of cells. (N) Quantification of nuclear *vs.* cytoplasmic distribution of Flag–Eya in experiments A, B, and F–I. *N* values are shown across the top of the graph. (O) Quantification of cytoplasmic Eya distribution into punctate structures in experiments A, B, and D–M. Punctate classification is a subset of membrane associated (*i.e.*, some cells categorized as having punctate staining also have membrane-associated staining). *N* values are shown across the top of the graph.

cytoplasmic activity was implied by the identified interactions (Okabe *et al.* 2009; Liu *et al.* 2012). Intriguingly, the Jak/Stat pathway is relevant to innate immunity in both *Drosophila* and mammals (reviewed in Agaisse and Perrimon 2004 and O'Shea and Plenge 2012). In *Drosophila*, Jak/Stat signaling regulates hemocyte (blood cell) development and release of Upd cytokines in response to infection (Agaisse *et al.* 2003; Copf *et al.* 2011; Minakhina *et al.* 2011; Woodcock *et al.* 2015). The

tyrosine kinases from our short list of candidates also have potential links to immunity. *shark* and *Src42A* are important for Draper-mediated glial phagocytosis of axonal debris (Ziegenfuss *et al.* 2008) which, if left uncleared, stimulates an immune response, and Src64B overexpression has been shown to be sufficient for inducing an immune response in larva (Williams 2009). Even if Eya's threonine phosphatase activity is not involved, extending exploration of the interactions we have uncovered in the context of axon guidance to other biological contexts in which the candidate interacting partner is known to function may provide new insight into the cytoplasmic signaling networks in which Eya participates during development and disease.

Acknowledgments

We thank Fangfang Jiang for being integral to this work by providing some data included in Figure 2A and for performing the experiments shown in Figure 5, E and F and Figure S3; J. F. Boisclair-Lachance, T. Davis, M. Hope, N. Sanchez, and J. Webber for comments on the manuscript; R. Fehon, E. Ferguson, M. Glotzer, R. Jones, and V. Prince for discussions; and E. Bach for reagents. C.S.L.H. was supported by National Institutes of Health (NIH) T32-GM07197 and by NIH R01-EY12549 (to I.R.). W.X. was supported by a Women's Board fellowship of the University of Chicago and by an American Heart Association predoctoral fellowship. Sequencing and monoclonal antibody costs were partially subsidized by the University of Chicago Cancer Center support grant P30CA014599.

Literature Cited

Agaisse, H., and N. Perrimon, 2004 The roles of JAK/STAT signaling in Drosophila immune responses. Immunol. Rev. 198: 72–82.

Agaisse, H., U. M. Petersen, M. Boutros, B. Mathey-Prevot, and N. Perrimon, 2003 Signaling role of hemocytes in Drosophila JAK/STAT-dependent response to septic injury. Dev. Cell 5: 441–450.

Almudi, I., I. Poernbacher, E. Hafen, and H. Stocker, 2013 The Lnk/SH2B adaptor provides a fail-safe mechanism to establish the Insulin receptor-Chico interaction. Cell Commun. Signal. 11: 26.

Arbouzova, N. I., and M. P. Zeidler, 2006 JAK/STAT signalling in Drosophila: insights into conserved regulatory and cellular functions. Development 133: 2605–2616.

Bach, E. A., L. A. Ekas, A. Ayala-Camargo, M. S. Flaherty, H. Lee *et al*., 2007 GFP reporters detect the activation of the Drosophila JAK/STAT pathway in vivo. Gene Expr. Patterns 7: 323–331.

Bayle, J., S. Letard, R. Frank, P. Dubreuil, and P. De Sepulveda, 2004 Suppressor of cytokine signaling 6 associates with KIT and regulates KIT receptor signaling. J. Biol. Chem. 279: 12249–12259.

Bonini, N. M., W. M. Leiserson, and S. Senzer, 1993 The eyes absent gene : genetic control of cell survival and differentiation in the developing Drosophila eye. Cell 72: 379–395.

Bonini, N. M., W. M. Leiserson, and S. Benzer, 1998 Multiple roles of the eyes absent gene in Drosophila. Dev. Biol. 196: 42–57.

Callus, B. A., and B. Mathey-Prevot, 2002 SOCS36E, a novel Drosophila SOCS protein, suppresses JAK/STAT and EGF-R signalling in the imaginal wing disc. Oncogene 21: 4812–4821.

Chao, J.-L., Y.-C. Tsai, S.-J. Chiu, and Y. H. Sun, 2004 Localized Notch signal acts through eyg and upd to promote global growth in Drosophila eye. Development 131: 3839–3847.

Chen, X. P., J. A Losman, and P. Rothman, 2000 SOCS proteins, regulators of intracellular signaling. Immunity 13: 287–290.

Cherbas, L., A Willingham, D Zhang, L Yang, Y Zou *et al*., 2011 The transcriptional diversity of 25 Drosophila cell lines. Genome Res. 21: 301–314.

Cook, P. J., B. G. Ju, F. Telese, X. Wang, C. K. Glass *et al.*, 2009 Tyrosine dephosphorylation of H2AX modulates apoptosis and survival decisions. Nature 458: 591–596.

Copf, T., V. Goguel, A. Lampin-Saint-Amaux, N. Scaplehorn, and T. Preat, 2011 Cytokine signaling through the JAK/STAT pathway is required for long-term memory in Drosophila. Proc. Natl. Acad. Sci. USA 108: 8059–8064.

Ekas, L. A., G. -H. Baeg, M. S. Flaherty, A. Ayala-Camargo, and E. A. Bach, 2006 JAK/STAT signaling promotes regional specification by negatively regulating wingless expression in Drosophila. Development 133: 4721–4729.

El-Hashash, A. H., G. Turcatel, and S. Varma, M. BerikaD. Al Alam *et al*., 2012 Eya1 protein phosphatase regulates tight junction formation in lung distal epithelium. J. Cell Sci. 125: 4036–4048.

Garrity, P. A., C.-H. Lee, I. Salecker, H. C. Robertson, C. J. Desai *et al.*, 1999 Retinal axon target selection in Drosophila is regulated by a receptor protein tyrosine phosphatase. Neuron 22: 707–717.

Gross, G. G., R. M. R. Feldman, A. Ganguly, J. Wang, H. Yu *et al.*, 2008 Role of X11 and ubiquilin as in vivo regulators of the amyloid precursor protein in Drosophila. PLoS One 3: e2495.

Gutierrez-Aviño, F. J., D. Ferres-Marco, and M. Dominguez, 2009 The position and function of the Notch-mediated eye growth organizer: the roles of JAK/STAT and four-jointed. EMBO Rep. 10: 1051–1058.

Hase, M., Y. Yagi, H. Taru, S. Tomita, A. Sumioka *et al.*, 2002 Expression and characterization of the Drosophila X11-like/Mint protein during neural development. J. Neurochem. 81: 1223–1232.

Heanue, T. A., R. Reshef, R. J. Davis, G. Mardon, G. Oliver *et al.*, 1999 Synergistic regulation of vertebrate muscle development by Dach2, Eya2, and Six1, homologs of genes required for Drosophila eye formation. Genes Dev. 13: 3231–3243.

Hing, H., J. Xiao, N. Harden, L. Lim, and S. L. Zipursky, 1999 Pak functions downstream of dock to regulate photoreceptor axon guidance in Drosophila. Cell 97: 853–863.

Hirose, T., B. D. Galvin, and H. R. Horvitz, 2010 Six and Eya promote apoptosis through direct transcriptional activation of the proapoptotic BH3-only gene egl-1 in Caenorhabditis elegans. Proc. Natl. Acad. Sci. USA 107: 15479–15484.

Housden, B. E., and N. Perrimon, 2014 Spatial and temporal organization of signaling pathways. Trends Biochem. Sci. 39: 457–464.

Jemc, J., and I. Rebay, 2007 The eyes absent family of phosphotyrosine phosphatases: properties and roles in developmental regulation of transcription. Annu. Rev. Biochem. 76: 513–538.

Jeon, M., H. Nguyen, S. Bahri, and K. Zinn, 2008 Redundancy and compensation in axon guidance: genetic analysis of the Drosophila Ptp10D/Ptp4E receptor tyrosine phosphatase subfamily. Neural Dev. 3: 3.

Jin, M., and G. Mardon, 2016 Distinct biochemical activities of eyes absent during Drosophila eye development. Sci. Rep. 6: 23228.

Jin, M., B. Jusiak, Z. Bai, and G. Mardon, 2013 Eyes absent tyrosine phosphatase activity is not required for Drosophila development or survival. PLoS One 8: e58818.

Kazi, J. U., J. Sun, B. Phung, F. Zadjali, A. Flores-Morales *et al.*, 2012 Suppressor of cytokine signaling 6 (SOCS6) negatively regulates Flt3 signal transduction through direct binding to phosphorylated tyrosines 591 and 919 of Flt3. J. Biol. Chem. 287: 36509–36517.

Koytiger, G., A. Kaushansky, A. Gordus, J. Rush, P. K. Sorger *et al.*, 2013 Phosphotyrosine signaling proteins that drive oncogenesis tend to be highly interconnected. Mol. Cell. Proteomics 12: 1204–1213.

Krishnan, N., D. G. Jeong, S.-K. Jung, S. E. Ryu, A. Xiao *et al.*, 2009 Dephosphorylation of the C-terminal tyrosyl residue of the DNA damage-related histone H2A.X is mediated by the protein phosphatase eyes absent. J. Biol. Chem. 284: 16066–16070.

Kumar, J. P., 2009 The molecular circuitry governing retinal determination. Biochim. Biophys. Acta 1789: 306–314.

Li, W. X., 2008 Canonical and non-canonical JAK-STAT signaling. Trends Cell Biol. 18: 545–551.

Li, W.-Z., S.-L. Li, H. Y. Zheng, S.-P. Zhang, and L. Xue, 2012 A broad expression profile of the GMR-GAL4 driver in Drosophila melanogaster. Genet. Mol. Res. 11: 1997–2002.

Li, X., K. A Oghi, J. Zhang, A. Krones, K. T. Bush *et al.*, 2003 Eya protein phosphatase activity regulates Six1-Dach-Eya transcriptional effects in mammalian organogenesis. Nature 426: 247–254.

Liu, X., T. Sano, Y. Guan, S. Nagata, J. A. Hoffmann *et al.*, 2012 Drosophila EYA regulates the immune response against DNA through an evolutionarily conserved threonine phosphatase motif. PLoS One 7: e42725.

Luo, H., H. Asha, L. Kockel, T. Parke, M. Mlodzik *et al.*, 1999 The Drosophila Jak kinase hopscotch is required for multiple developmental processes in the eye. Dev. Biol. 213: 432–441.

Minakhina, S., W. Tan, and R. Steward, 2011 JAK/STAT and the GATA factor Pannier control hemocyte maturation and differentiation in Drosophila. Dev. Biol. 352: 308–316.

Ngo, K. T., J. Wang, M. Junker, S. Kriz, G. Vo *et al.*, 2010 Concomitant requirement for Notch and Jak/Stat signaling during neuroepithelial differentiation in the Drosophila optic lobe. Dev. Biol. 346: 284–295.

Nica, G., W. Herzog, C. Sonntag, M. Nowak, H. Schwarz *et al.*, 2006 Eya1 is required for lineage-specific differentiation, but not for cell survival in the zebrafish adenohypophysis. Dev. Biol. 292: 189–204.

Nicholson, S. E., T. A. Willson, A. Farley, R. Starr, J. G. Zhang *et al.*, 1999 Mutational analyses of the SOCS proteins suggest a dual domain requirement but distinct mechanisms for inhibition of LIF and IL-6 signal transduction. EMBO J. 18: 375–385.

O'Shea, J. J., and R. Plenge, 2012 JAK and STAT signaling molecules in immunoregulation and immune-mediated disease. Immunity 36: 542–550.

Oh, S. T., E. F. Simonds, C. Jones, M. B. Hale, Y. Goltsev *et al.*, 2010 Novel mutations in the inhibitory adaptor protein LNK drive JAK-STAT signaling in patients with myeloproliferative neoplasms. Blood 116: 988–992.

Ohto, H., S. Kamada, K. Tago, H. Ozaki, and S. Sato, 1999 Cooperation of Six and Eya in activation of their target genes through nuclear translocation of Eya. Mol. Cell. Biol. 19: 6815–6824.

Okabe, Y., T. Sano, and S. Nagata, 2009 Regulation of the innate immune response by threonine-phosphatase of Eyes absent. Nature 460: 520–524.

Oliva, C., and J. Sierralta, 2010 Regulation of axonal development by the nuclear protein hindsight (pebbled) in the Drosophila visual system. Dev. Biol. 344: 911–921.

Piessevaux, J., D. Lavens, F. Peelman, and J. Tavernier, 2008 The many faces of the SOCS box. Cytokine Growth Factor Rev. 19: 371–381.

Pignoni, F., B Hu, K. H Zavitz, J Xiao, P. A Garrity *et al.*, 1997 The eye-specification proteins So and Eya form a complex and regulate multiple steps in Drosophila eye development. Cell 91: 881–891.

Rajan, A., and N. Perrimon, 2012 Drosophila cytokine unpaired 2 regulates physiological homeostasis by remotely controlling insulin secretion. Cell 151: 123–137.

Rawlings, J. S., K. M Rosler, and D. A Harrison, 2004a The JAK/STAT signaling pathway. J. Cell Sci. 117: 1281–1283.

Rawlings, J. S., G Rennebeck, S. M. W Harrison, R Xi, and D. A Harrison, 2004b Two Drosophila suppressors of cytokine signaling (SOCS) differentially regulate JAK and EGFR pathway activities. BMC Cell Biol. 5: 38.

Rayapureddi, J. P., C. Kattamuri, B. D. Steinmetz, B. J. Frankfort, E. J. Ostrin *et al.*, 2003 Eyes absent represents a class of protein tyrosine phosphatases. Nature 426: 295–298.

Schindelholz, B., M. Knirr, R. Warrior, and K. Zinn, 2001 Regulation of CNS and motor axon guidance in Drosophila by the receptor tyrosine phosphatase DPTP52F. Development 128: 4371–4382.

De Sepulveda, P., K. Okkenhaug, J. L. Rose, R. G. Hawley, P. Dubreuil *et al.*, 1999 Socs1 binds to multiple signalling proteins and suppresses steel factor-dependent proliferation. EMBO J. 18: 904–915.

Silver, S. J., and I. Rebay, 2005 Signaling circuitries in development: insights from the retinal determination gene network. Development 132: 3–13.

Slack, C., C. Werz, D. Wieser, N. Alic, A. Foley *et al.*, 2010 Regulation of lifespan, metabolism, and stress responses by the Drosophila SH2B protein, Lnk. PLoS Genet. 6: e1000881.

Song, J. K., R. Kannan, G. Merdes, J. Singh, M. Mlodzik *et al.*, 2010 Disabled is a bona fide component of the Abl signaling network. Development 137: 3719–3727.

Tadjuidje, E., and R. S. Hegde, 2013 The Eyes Absent proteins in development and disease. Cell. Mol. Life Sci. 70: 1897–1913.

Tootle, T. L., and S. J. Silver, E. L Davies, V Newman, R. R Latek *et al.*, 2003 The transcription factor Eyes absent is a protein tyrosine phosphatase. Nature 426: 299–302.

Trengove, M. C., and A. C. Ward, 2013 SOCS proteins in development and disease. Am. J. Clin. Exp. Immunol. 2: 1–29.

Tsai, Y.-C., and Y. H. Sun, 2004 Long-range effect of upd, a ligand for Jak/STAT pathway, on cell cycle in Drosophila eye development. Genesis 39: 141–153.

Voas, M. G., and I. Rebay, 2004 Signal integration during development: insights from the Drosophila eye. Dev. Dyn. 229: 162–175.

Wang, W., Y. Li, L. Zhou, H. Yue, and H. Luo, 2011 Role of JAK/STAT signaling in neuroepithelial stem cell maintenance and proliferation in the Drosophila optic lobe. Biochem. Biophys. Res. Commun. 410: 714–720.

Werz, C., K. Köhler, E. Hafen, and H. Stocker, 2009 The Drosophila SH2B family adaptor Lnk acts in parallel to chico in the insulin signaling pathway. PLoS Genet. 5: e1000596.

Williams, M. J., 2009 The c-src homologue Src64B is sufficient to activate the Drosophila cellular immune response. J. Innate Immun. 1: 335–339.

Woodcock, K. J., K. Kierdorf, C. A. Pouchelon, V. Vivancos, M. S. Dionne *et al.*, 2015 Macrophage-derived upd3 cytokine causes impaired glucose homeostasis and reduced lifespan in Drosophila fed a lipid-rich diet. Immunity 42: 133–144.

Xiong, W., N. M. Dabbouseh, and I. Rebay, 2009 Interactions with the Abelson tyrosine kinase reveal compartmentalization of eyes absent function between nucleus and cytoplasm. Dev. Cell 16: 271–279.

Xu, J., E. Y. M. Wong, C. Cheng, J. Li, M. T. K. Sharkar *et al.*, 2014 Eya1 interacts with Six2 and Myc to regulate expansion

of the nephron progenitor pool during nephrogenesis. Dev. Cell 31: 434–447.
Zeidler, M. P., N. Perrimon, and D. I. Strutt, 1999 Polarity determination in the Drosophila eye: a novel role for unpaired and JAK/STAT signaling. Genes Dev. 13: 1342–1353.
Zhu, F., H. Ding, and B. Zhu, 2013 Transcriptional profiling of Drosophila S2 cells in early response to Drosophila C virus. Virol. J. 10: 210.
Ziegenfuss, J. S., R. Biswas, M. A. Avery, K. Hong, A. E. Sheehan *et al.*, 2008 Draper-dependent glial phagocytic activity is mediated by Src and Syk family kinase signalling. Nature 453: 935–939.
Zou, D., D. Silvius, B. Fritzsch, and P.-X. Xu, 2004 Eya1 and Six1 are essential for early steps of sensory neurogenesis in mammalian cranial placodes. Development 131: 5561–5572.

Communicating editor: M. F. Wolfner

GENETICS

Supporting Information
www.genetics.org/lookup/suppl/doi:10.1534/genetics.115.185918/-/DC1

Retinal Axon Guidance Requires Integration of Eya and the Jak/Stat Pathway into Phosphotyrosine-Based Signaling Circuitries in *Drosophila*

Charlene S. L. Hoi, Wenjun Xiong, and Ilaria Rebay

DOI: 10.1534/genetics.115.185918

Supplemental Figure S1

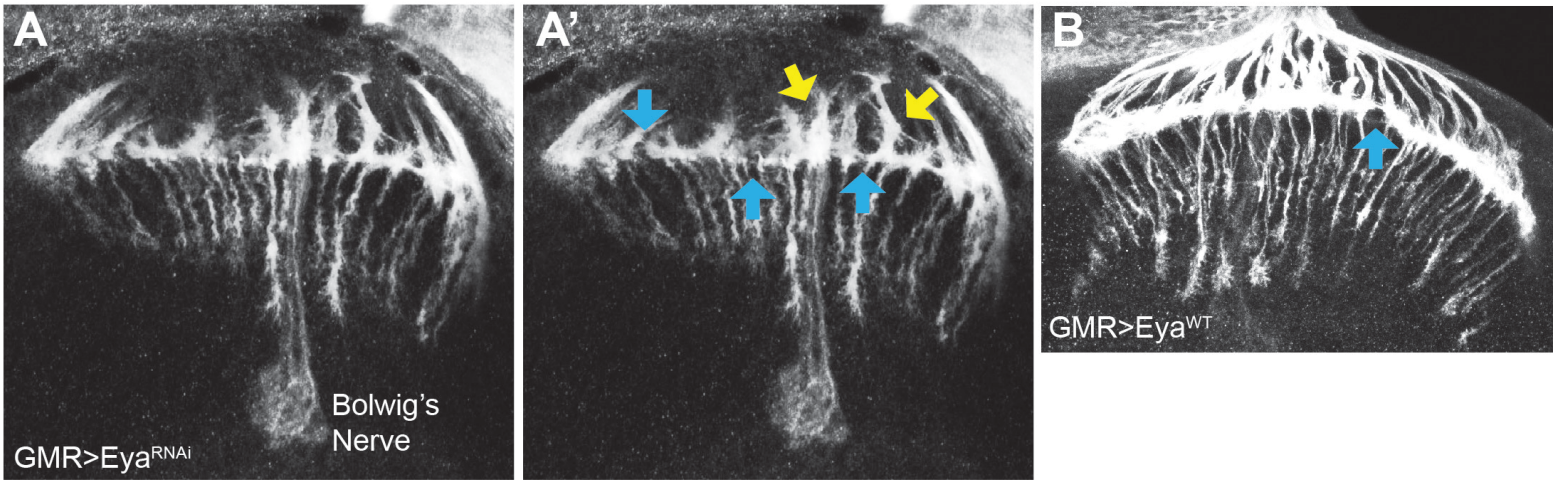

Figure S1 | Comparison of *eya* knockdown versus overexpression axon guidance phenotype

(A) *GMR>Eya*^{RNAi} animals have brains with thick axon fascicles (highlighted in A' by yellow arrows) and an uneven lamina plexus with frequent gaps highlighted in A' by blue arrows. (B) In contrast, *GMR>Eya*^{WT} animals only occasionally have disruptions to the lamina plexus (blue arrow).

Supplemental Figure S2

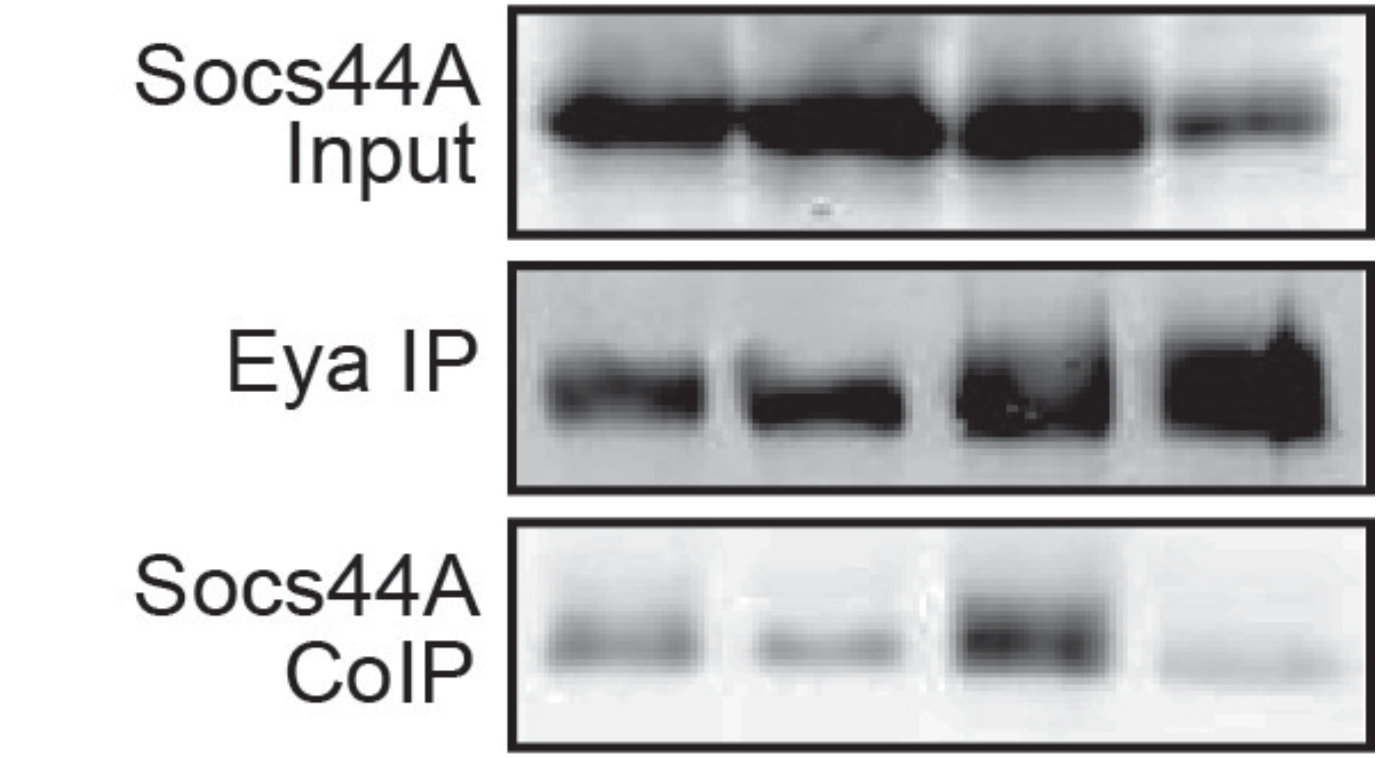

Eya	+	+	+	+
Abl			+	+
$Socs44A^{WT}$	+		+	
$Socs44A^{SH2*}$		+		+

Figure S2 | A missense mutation in the Socs44A SH2 domain disrupts CoIP with pY-Eya

Western blot showing that Flag-Eya co-transfected with Abl only weakly CoIPs HA-Socs44A^{SH2*}(Socs44A^{R214K}). Top panel, blotted with anti-HA, shows input levels for Socs44A constructs. Middle panel, blotted with anti-Flag, shows IP of Flag-tagged Eya. Bottom panel shows CoIP of WT, but not SH2 mutated, Socs44A with Eya when Abl is cotransfected.

Supplemental Figure S3

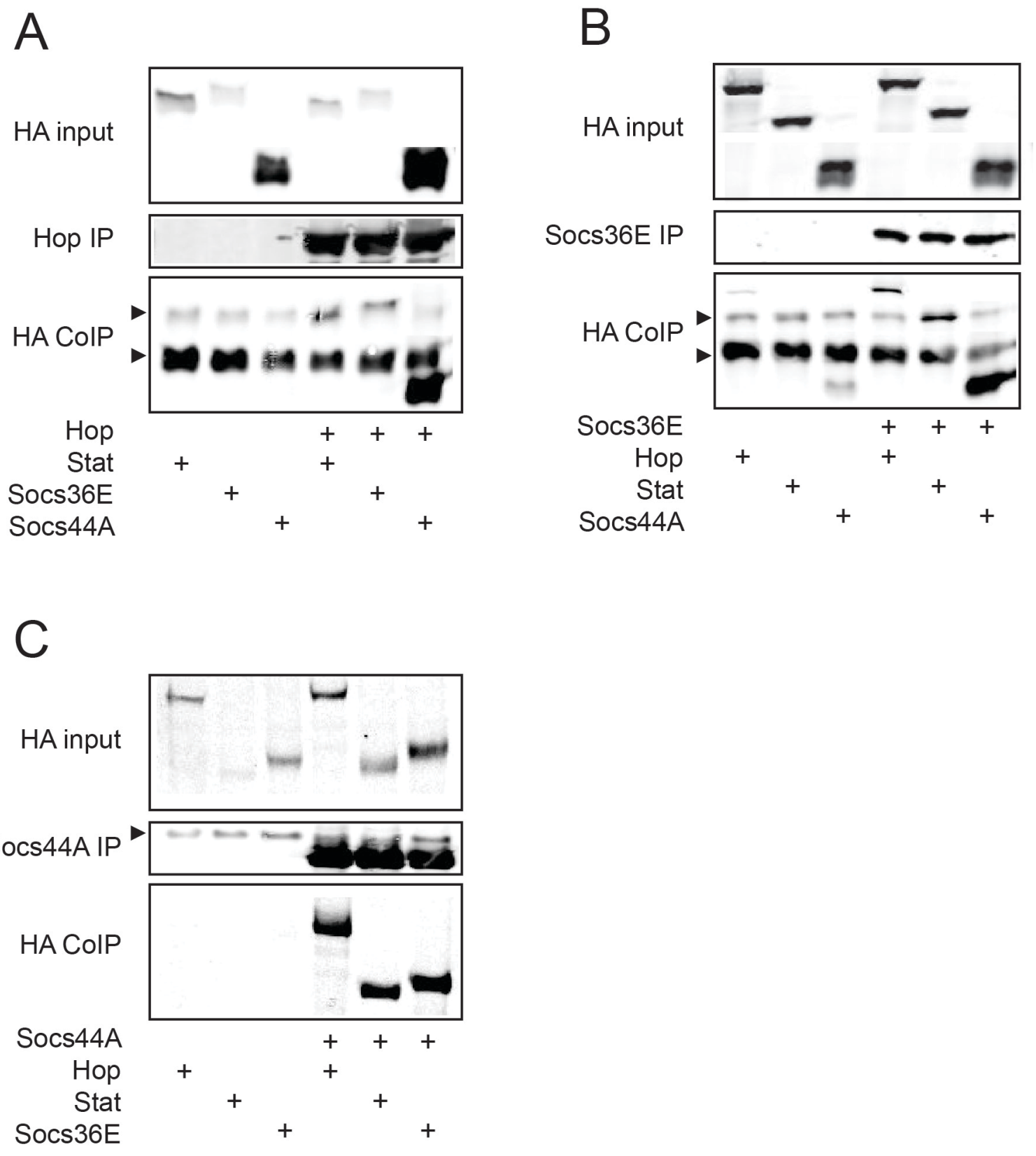

Figure S3 | Jak/Stat components CoIP each other

(A-C) Western blots showing CoIP results from transfected Drosophila S2 cells. Top panels, blotted with anti-HA, show input levels for the HA-tagged Jak/Stat genes. Middle panels, blotted with anti-Flag, show IP of Flag-tagged Jak/Stat genes. Bottom panels show CoIP of HA-tagged Jak/Stat genes. Key below indicates factors transfected in each experiment. Black triangles mark IgG bands. Stat and Socs36E both run very close to IgG heavy chain while Socs44A runs below IgG light chain. (A) Flag-Hop CoIPs HA-Stat, HA-Socs36E and HA-Socs44A. (B) Flag-Socs36E CoIPs HA-Hop, HA-Stat and HA-Socs44A. (C) Flag-Socs44A CoIPs HA-Hop, HA-Stat and HA-Socs36E.

Supplemental Figure S4

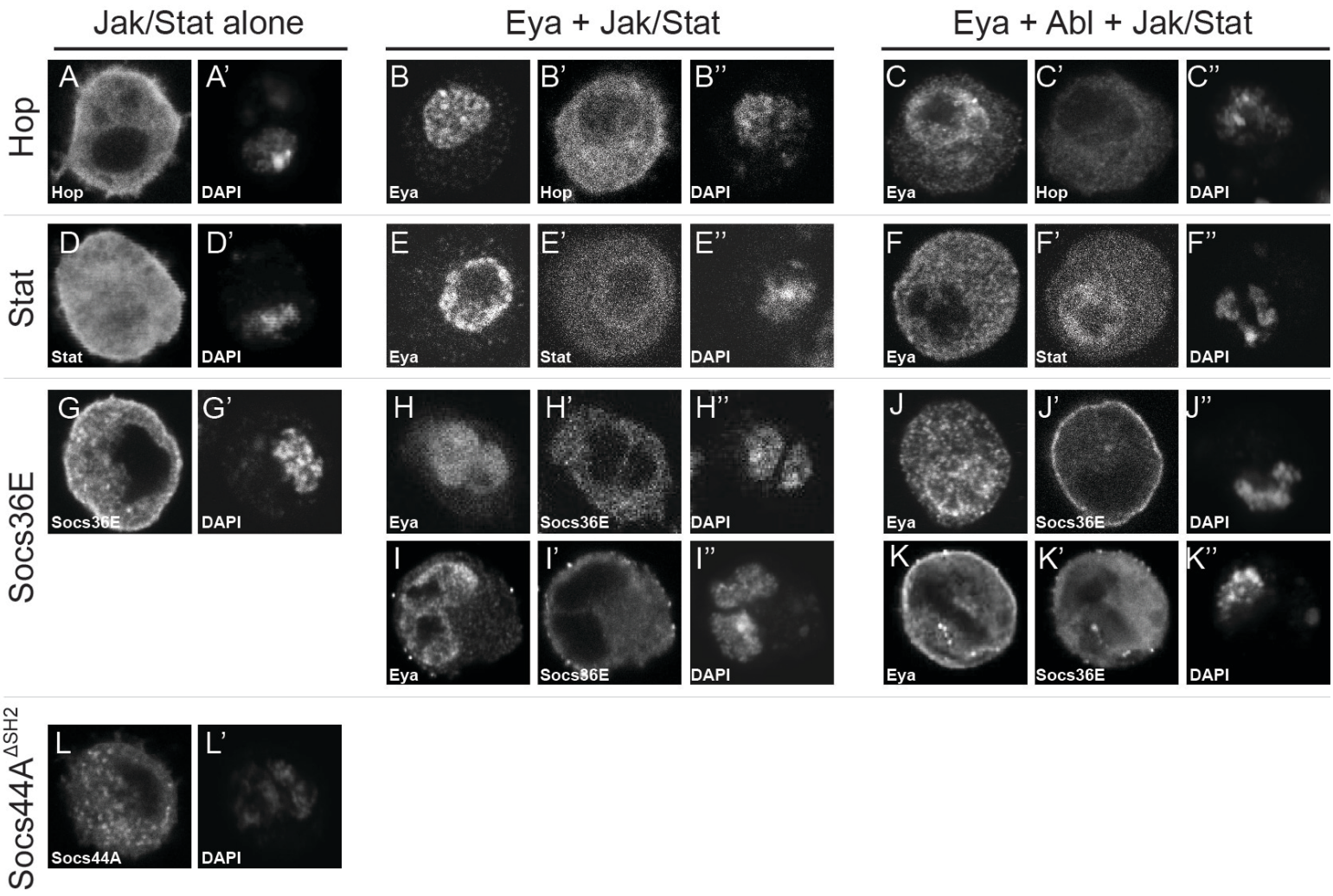

Figure S4 | Subcellular localization of Hop, Stat or Socs36E in S2 cells co-transfected with Eya or with Eya and Abl, and Socs44A$^{\Delta SH2}$

(A-N) Individual transfected S2 cells showing representative subcellular distribution of HA-tagged Jak/Stat genes and Flag-Eya. Nuclei are marked with DAPI. (A-C) Hop localization is predominantly cytoplasmic and becomes subtly nuclear upon co-transfection of Eya. (A) HA-Hop is exclusively cytoplasmic. Co-transfection of Eya (B) or Eya and Abl (C) enables detection of HA-Hop in the nucleus. Hop's mammalian orthologs, Jak1 and Jak2, do localize to the nucleus (Lobie *et al.* 1996; Ram and Waxman 1997). Eya localization is unaffected by co-transfection of Hop (B) and still relocalizes to the cytoplasm with co-transfection of Abl and Hop (C). (D-H) Stat localizes throughout the cell and becomes more nuclear with co-transfection of either Eya or Eya and Abl. (D) HA-Stat localizes to both the nucleus and cytoplasm. (E-F) Two representative cells showing that co-transfection of Eya will cause HA-Stat to become more nuclear while Flag-Eya localization is unchanged. (G-H) Two representative cells showing that co-transfection of Eya, Abl and Stat results in HA-Stat becoming more nuclear but Flag-Eya still relocalizes to the cytoplasm. (I-M) HA-Socs36E is exclusively cytoplasmic with some membrane-association. (J-K) Two representative cells showing that co-transfection of Socs36E does not induce dramatic redistribution of Flag-Eya (J), although some instances of cytoplasmic Eya accumulating into puncta are observed (K). (L) HA-Socs44A$^{\Delta SH2}$ is heterogeneously distributed throughout the cytoplasm. This localization does not change with co-transfection of Eya (Figure 6J) or Eya and Abl (Figure 6K).

		RNAi element	GMR>Eya^{WT}		n	GMR>Eya^{RNAi}		n	GMR>Myr-Eya^{WT}		n	GMR>NLS-Eya^{WT}		n
		none (w^{1118})	25.7 ± 6.1		11	18.8 ± 2.5		33	18.9 ± 5.0		65	26.6 ± 4.9		64
SH2 domain	Jak/Stat Signaling	hop^{40037}	22.4 ± 4.8		26									
		hop^{102830}	16.6 ± 6.8***	↓	42	23.2 ± 5.1*	↑	11	14.3 ± 6.2*	↓	17	39.8 ± 6.6***	↑	9
		Stat92E^{43866}	19.8 ± 2.6*	↓	16	21.1 ± 3.3*	↑	24	13.6 ± 4.5**	↓	5	31.6 ± 4.9**	↑	5
		Stat92E^{106980}	19.3 ± 6.1*	↓	12	25.0 ± 3.7***	↑	16	12.9 ± 4.8***	↓	19	42.3 ± 7.3***	↑	21
		Socs36E^{51821}	22.3 ± 3.8		19									
		Socs36E^{52192}	17.7 ± 4.4**	↓	9	22.0 ± 4.4*	↑	16	11.2 ± 4.1***	↓	14	27.5 ± 7.6		11
		Socs44A^{33489}	25.4 ± 3.8		16									
		Socs44A^{102764}	14.3 ± 5.3***	↓	32	21.0 ± 4.0*	↑	61	12.1 ± 7.3**	↓	14	40.7 ± 3.5***	↑	20
		Socs16D^{48210}	22.4 ± 3.3		25									
		Socs16D^{100566}	21.4 ± 4.4		27									
	Insulin Signaling	Lnk^{32892}	22.6 ± 3.3		21									
		Lnk^{103646}	13.4 ± 6.5***	↓	33	23.3 ± 4.6*	↑	11	12.6 ± 5.3***	↓	34	45.3 ± 6.0***	↑	20
		Pi3k21B^{33556}	22.1 ± 5.2		19									
		Pi3k21B^{104179}	23.0 ± 4.8		8									
	SH3 domain	Crk^{19061}	27.1 ± 8.3		14									
		Crk^{106496}	20.9 ± 3.7*	↓	15									
		dock^{37524}	26.1 ± 2.8		16									
		dock^{107064}	24.9 ± 4.1		12									
		drk^{105498}	22.5 ± 5.2		8									
		sl^{7173}	21.9 ± 5.3		10									
		sl^{7174}	21.5 ± 6.4		15									
		vap^{44638}	20.2 ± 5.7*	↓	18									
		vap^{107341}	17.9 ± 5.9**	↓	30	17.1 ± 2.9*	↓	15						
		Vav^{6241}	21.1 ± 3.4*	↓	10									
		Vav^{103820}	23.3 ± 3.4		12									
	Tyrosine Kinase	Btk29A^{22675}	23.6 ± 3.1		4									
		Btk29A^{106962}	22.5 ± 2.7		11									
		Src42A^{100708}	12.7 ± 4.3***	↓	25	21.3 ± 4.0*	↑	25	10.6 ± 5.1***	↓	25	36.1 ± 5.4***	↑	19
		Src64B^{35252}	15.5 ± 2.9***	↓	22	22.8 ± 3.8***	↑	19	9.8 ± 3.2***	↓	22	20.2 ± 4.9***	↓	18
		Csk^{32877}	16.7 ± 4.0***	↓	16	24.5 ± 4.7***	↑	31	12.1 ± 5.2***	↓	36	41.0 ± 6.5**	↑	20
		Fps85D^{36053}	23.0 ± 2.4		6									
		Fps85D^{107266}	22.0 ± 3.5		11									
		shark^{25304}	17.2 ± 4.7***	↓	22	23.3 ± 2.3***	↑	18	10.3 ± 3.8***	↓	23	36.8 ± 4.5***	↑	12
		shark^{105706}	18.4 ± 3.1**	↓	12	16.1 ± 3.4**	↓	21						
		csw^{21756}	18.6 ± 4.7**	↓	12	24.5 ± 3.4***	↑	10	19.9 ± 6.2		19	20.0 ± 4.4***	↓	20
		csw^{21757}	22.7 ± 2.9		13									
		PVRAP^{26046}	24.2 ± 4.8		17									
		RhoGAP5A^{41779}	23.9 ± 4.6		9									
		RhoGAP5A^{41780}	23.5 ± 4.2		10									
		RhoGAP5A^{102000}	23.2 ± 3.8		9									
		spri^{25140}	21.9 ± 3.2		3									
		spri^{101164}	23.2 ± 4.3		11									
		CG9098^{27001}	23.5 ± 4.5		15									
		CG10479^{45098}	20.7 ± 4.5*	↓	27									
		CG10479^{106226}	21.3 ± 4.1*	↓	21									
		CG11146^{47795}	23.7 ± 6.0		22									
		CG11146^{101324}	20.9 ± 3.6*	↓	8									
		CG15529^{50228}	21.8 ± 7.7		24									
		CG15529^{100438}	17.9 ± 2.8**	↓	14	18.8 ± 2.6		12						
		CG33993^{40702}	22.1 ± 6.6		23									
		CG33993^{102754}	21.0 ± 7.1		8									
	PTB domain	by^{22823}	28.7 ± 3.9		19									
		Shc^{40464}	20.5 ± 6.8*	↓	29									
		Shc^{103906}	20.3 ± 3.5*	↓	19									
		ced-6^{16313}	21.8 ± 3.6		13									
		Dab^{13005}	18.1 ± 6.7**	↓	13	23.6 ± 2.9***	↑	21	14.8 ± 3.5**	↓	11	13.7 ± 3.6***	↑	12
		Dab^{14008}	13.0 ± 4.3***	↓	36	24.0 ± 2.7***	↑	16	11.8 ± 2.7***	↓	9	25.7 ± 5.0		12
		plx^{27335}	6.54 ± 3.1***	↓	13	19.8 ± 3.3		21						
		plx^{106969}	26.6 ± 4.5		15									
		X11L^{27479}	13.5 ± 4.4***	↓	23	24.7 ± 5.1*	↑	9	11.1 ± 4.4***	↓	28	34.8 ± 4.6***	↑	22
		X11Lβ^{8309}	10.4 ± 5.1***	↓	23	21.8 ± 3.9*	↑	12	19.8 ± 6.0		12	33.4 ± 4.2***	↑	18
		X11Lβ^{14872}	27.4 ± 5.8		9									
		CG4393^{105381}	23.6 ± 4.1		10									

TABLE S1

Table S1 | Complete genetic screen results.

Complete results from the primary and secondary genetic screens. SH2/PTB genes are grouped into known categories of signaling and superscripted numbers indicate the VDRC line. All lines were crossed to *GMR>Eya^{WT};RTL* for the primary screen, and hits were subsequently crossed to *GMR>Eya^{RNAi};RTL*, *GMR>Myr-Eya^{WT};RTL*, and *GMR>NLS-Eya^{WT};RTL* for secondary tests. Data shown in each column are averages of overshooting axons per brain with standard deviation, followed by p-value (* p-value <0.05, ** p-value < 0.01, *** p-value < 0.001), followed by an arrow indicating the direction of the genetic interaction (solid black down arrows mark significant suppression; open up arrows mark enhancement), followed by the number (N) of brains scored.